

I give permission for public access to my thesis and for any copying to be done at the discretion of the archives librarian and/or the College librarian.

ISOLATION AND CHARACTERIZATION OF  
LIPOPOLYSACCHARIDES FROM STRAINS OF ESCHERICHIA COLI  
AND THEIR IMPACT ON PREDATION BY THE BACTERIA  
*BDELLOVIBRIO BACTERIOVORUS*

By

Catherine Burke Volle

A thesis submitted to the faculty of Mount Holyoke College in partial  
fulfillment of the requirements for the degree of Bachelor of Arts with honors

Program in Biochemistry

Mount Holyoke College

South Hadley, MA

May, 2006

This paper was prepared  
under the direction of Dr.  
Megan Nunez for 12 credits.

## ACKNOWLEDGEMENTS

First, I would like to thank Dr. Megan Nunez for her continued support and guidance in both this project and many other matters. Without your optimism, I never would have made it to this point.

Thank you to Dr. Jeff Knight, Dr. Thorsteinn Adalsteinsson, Dr. Lilian Hsu, and Dr. Craig Woodard for all their help, advice, and mental butt-kickings (especially Lilian). Also thank you to Dr. Sean Decatur for making my first college chemistry experience a great one. I would not have done this research if I had not enjoyed that first class. Thank you to the biology, biochemistry, and chemistry department for supplies.

I want to thank my parents for their continued love and support, even though they don't always know what I'm talking about.

Lastly I have to thank my lab mates (and I include Aragorn as he keeps people away from the windows), both past and present, for being wonderful people and wonderful friends. Anne, thanks for commiserating with me and giving me advice, and letting me plan your wedding. Amber, thank you for your assurance and ice cream trips. Amy, you are a wonderful friend and I'm glad I get to spend another year in lab with you.

**TABLE OF CONTENTS**

	Page
List of Figures	vii
Abstract	ix
Chapter 1: Introduction	
Section 1: <i>Bdellovibrio bacteriovorus</i>	1
Section 2: The Gram-Negative Cell Wall	8
Section 3: Purpose	16
Section 4: Supported Lipid Membranes	17
Chapter 2: Materials and Methods	
Section 1: Growth and Characterization of <i>Bdellovibrio</i>	24
Section 2: Prey Cell Selection	25
Section 3: LPS Extraction	26
Section 4: SDS-PAGE and Agarose Gel Electrophoresis	29
Section 5: Formation of Supported Lipid Membranes	31
Section 6: AFM Observations	34
Chapter 3: Results	
Section 1: <i>Bdellovibrio</i> Characterization and Predation of <i>E. coli</i> Strains O111:B4 and K12	36
Section 2: Developing a Method for LPS Preparation	42

Section 3: Comparison of Bacterial LPS Types	62
Section 4: Supported Lipid Monolayers	62
Chapter 4: Discussion	
Section 1: Bdellovibrio Cultivation	84
Section 2: LPS Extraction and Purification	87
Section 3: LPS Characterization	92
Section 4: Supported LPS Monolayers	95
Chapter 5: Conclusions and Future Work	
Section 1: Conclusions and Future Work	102
References	105

**LIST OF FIGURES**

		Page
Figure 1	Growth Cycle of <i>Bdellovibrio bacteriovorus</i>	2
Figure 2	Diagram of the Gram-negative Bacterium Cell Wall	9
Figure 3	Schematic Drawing of a Generic <i>E. coli</i> Type LPS Molecule	10
Figure 4	LPS of <i>Bdellovibrio bacteriovorus</i> HD100	13
Figure 5	LPS of <i>E. coli</i> K12 W3100	15
Figure 6	Schematic Supported Lipid Monolayers	20
Figure 7	Schematic of AFM Function	22
Figure 8	<i>Bdellovibrio</i> Growing Within a ML35 Prey Cell	37
Figure 9	Cell Counts	40
Figure 10	Sepharose Column Fractions	44
Figure 11	Protein, DNA, and LPS for the ML35 Extraction Process	45
Figure 12	Protein, DNA, and LPS for the <i>Bdellovibrio</i> Extraction Process	49
Figure 13	Protein, DNA, and LPS for the ZK1056 Extraction Process	52
Figure 14	Protein, DNA, and LPS for the K12 Extraction Process	57

Figure 15	Protein, DNA, and LPS for the O111:B4 Extraction Process	60
Figure 16	Gel Showing Six Different LPS	63
Figure 17	Clean Glass Imaged With Contact AFM	65
Figure 18	AFM Images of Alkylated Glass	66
Figure 19	AFM Image of PC Monolayer	68
Figure 20	AFM Images of “Heads Up” Smooth LPS Monolayers	70
Figure 21	AFM Image of a Scratched LPS Monolayer	72
Figure 22	AFM Image of “Heads Up” Lipid A Monolayer	73
Figure 23	AFM Images of “Heads Up” Rough LPS Monolayers	75
Figure 24	AFM Image of Mica	76
Figure 25	AFM Images of “Tails Up” Rough LPS Monolayers	77
Figure 26	AFM Images of “Tails Up” Smooth LPS Monolayers	80
Figure 27	AFM Image of “Tails Up” Lipid A Monolayer	83

## ABSTRACT

The predatory bacterium *Bdellovibrio bacteriovorus* 109J grows inside its prey by absorbing nutrients from the prey cell's cytoplasm. An amazing aspect of the bdellovibrio life cycle is that while it consumes a wide spectrum of other Gram-negative bacteria, it is Gram-negative itself but does not eat other bdellovibrios. The outer membrane of both the predator and prey cells representing the exterior surface of the cell, is largely composed of lipopolysaccharide (LPS) molecules built of four main components: the lipid A base, the inner and outer core oligosaccharides, and the repeating O-antigen. It is likely a difference is present in the chemical structure or physical properties of the molecule that aids in the distinction of prey and non-prey cells by bdellovibrio, but it is not known what that difference is.

In order to examine the chemical and physical properties of the LPS of the bdellovibrios and several prey strains, the LPS molecules were first isolated from living predator or prey cells using a multi-step phenol extraction and differential centrifugation process that exploited the amphipathic nature of the molecules to purify the LPS from other biomolecules. The lipid A moieties were then isolated from the LPS using acid hydrolysis. Several different strains of *E. coli* were selected for study; these included O111:B4, a smooth strain isolated in a medical setting and used for various

microbiological studies, ZK1056, a biofilm-forming lab strain, ML35, a lab strain used in genetic studies, and K12, a rough strain that is commonly used in *Bdellovibrio* studies.

Once the LPS were isolated, they were characterized on polyacrylamide gels and stained with silver to highlight the O-antigens, with one band relating to each antigen unit. These data indicate that the *E. coli* prey K12 and ZK1056 are rough strains having no O-antigens, and ML35 and O111:B4 are smooth and have multiple O-antigen units. *Bdellovibrio bacteriovorus* 109J is a smooth strain and is similar to the ML35 in the overall size of the LPS.

The LPS were used to create model cell exteriors in the form of supported monolayers. These were characterized by contact atomic force microscopy (AFM). Monolayers were prepared on alkylated glass cover slips with the O-antigen or core (or lipid head in the case of lipid A) facing into solution and were imaged in aqueous buffer. These monolayers proved to be uniform, regardless of whether the LPS was designated as rough or smooth. All the monolayers were very fluid. When attempting to create a permanent hole in the monolayer, the LPS molecules would move back into place before an image could be obtained.

Monolayers were also prepared on freshly cleaved mica with the lipid tails facing out. These surfaces were imaged by AFM in air. These monolayers were considerably less fluid because the LPS were unable to

move on the mica. Interestingly, the smooth and rough strains had significantly different monolayers. The smooth LPS monolayers were even and uniform, whereas the rough LPS monolayers contained variable sized domains that may contain a higher molecular density than the surrounding monolayer. Since *bdellovibrio* LPS monolayers look like the other smooth strains, this difference in domain structure alone cannot explain the difference in predation.

This work is just the beginning of the characterization of these molecules; further experiments with a Langmuir-Blodgett trough will allow us to control the LPS density and molecular packing in these monolayers as well as measure the phase transitions and strength of intermolecular interactions. We expect that we will see a difference in the intermolecular interactions of the *bdellovibrio* LPS though not necessarily in the gross morphology of monolayers that are formed. Further experiments based on those performed by other groups will focus on chemical differences in the head groups of the prey and predator LPS lipid A and the differences these produce in the physical properties of the model membranes, which may provide the key to determining how *bdellovibrios* select their prey.

## CHAPTER 1: INTRODUCTION

### Section 1: *Bdellovibrio bacteriovorus*

*Bdellovibrio bacteriovorus* is a predatory Gram-negative bacterium first reported by Stolp and Starr in 1963. The bacterium itself is vibroid shaped and has a flagellum at one end. It is a small bacterium, only about 0.25 to 0.40  $\mu\text{m}$  in width and 1 to 2  $\mu\text{m}$  in length. It is characterized by a two phase life cycle. In the attack phase, the bdellovibrio must bind and enter the prey cell. Once the bdellovibrio has entered, the prey cell changes shape and is referred to as a bdelloplast. During the growth phase, the bdellovibrio obtains nutrients from the cytoplasm of the prey cell while it elongates. Eventually the bdellovibrio divides into progeny cells which develop flagella and burst from the prey cell (Fig. 1) (1). *Bdellovibrio* can also grow outside of a prey bacterium in a process called anoxic growth. In this cycle a similar growth pattern is followed without the added protection and nutrients of a prey bacterium. This host independence is a mutation induced in a laboratory and anoxic strains are not found in nature (2).

The intracellular life cycle of the *Bdellovibrio bacteriovorus* 109J begins when it recognizes and binds to its prey. It finds its prey by randomly swimming into it; *Bdellovibrio bacteriovorus* UKi2 shows little to no

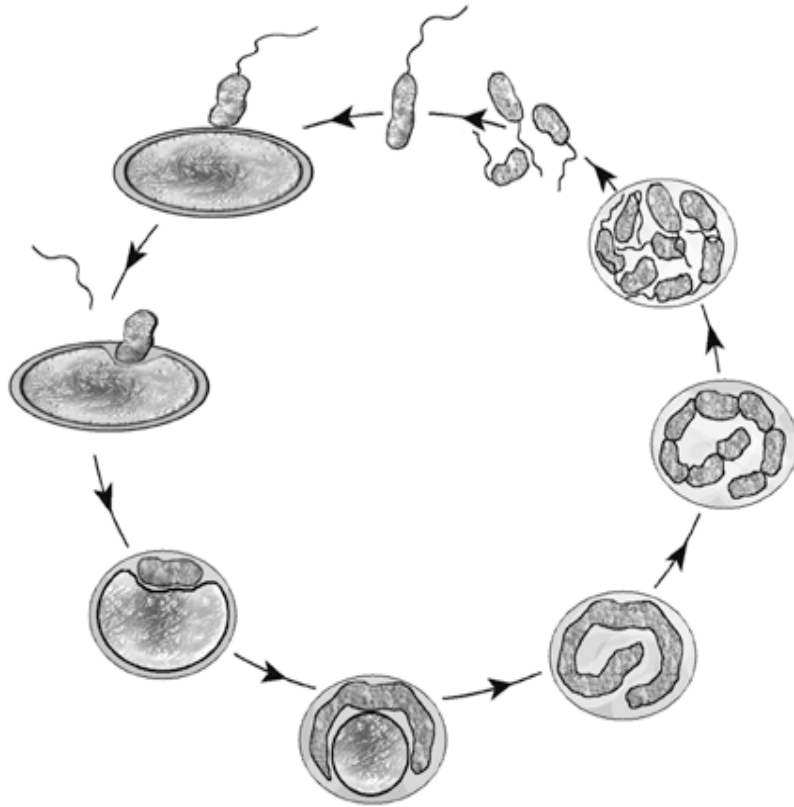


Figure 1: Growth cycle of *Bdellovibrio bacteriovorus*. This intraperiplasmic growth cycle is characterized by the penetration into the prey cell by the *bdellovibrio* (top left), the rounding of the prey cell into the "bdelloplast" (bottom left), the growth in the periplasmic space (bottom and right), and finally the release of the progeny cells to start the cycle again (top right). Image provided by Dr. J. Quinn.

chemotaxis to various pure compounds (3), amino acids (4), or entire prey cells (5). At first contact, the cell wall of the bdellovibrio is pressed flat against the cell wall of the prey cell. At this point the prey cell looks no different from other prey cells around it (6). This binding is reversible; the bdellovibrios can leave the prey cell and attach to another. Reversible attachment does not prevent other bdellovibrios from entering the original prey cell. Some movement of the cells is observed due to the impact of the bdellovibrio hitting the prey (7). Bdellovibrios can bind and infect the prey cell whether or not the bacterium has a capsule, a structure that surrounds some Gram-negative bacteria and offers additional protection from the environment, specifically some antibacterial agents (8).

After reversible binding, irreversible binding is achieved in a process that is not very well understood. Subsequently, the first noticeable change in the prey cell structure is a bulging at the point of attachment. The cytoplasm is not disrupted by this attachment during irreversible binding, though the cytoplasmic membrane may pull away from the cell wall (9). While the irreversible binding step has been observed with microscopy, it is not yet known what causes the bdellovibrio to make the transition from reversible to irreversible binding. Early studies showed that there are several factors that will affect the ability of bdellovibrio to bind to its prey. Chelating agents, organic acids, phenol, low pH, and sodium chloride all substantially suppress bdellovibrio growth. There are also several factors that contribute to a high

binding rate, and thus a high predation rate. If the predator to host ratio is lowered, the number of bdellovibrios that are found attached to prey cells at a given time will increase. Studies have also shown that the highest attachment rate is achieved in dilute nutrient broth (DNB) and when incubated at a temperature of 30-35 degrees Celsius. A properly shaken mixture will also have a greater rate of attachment (10).

After the irreversible attachment, enzymatic activity begins to break the cross-links of the peptidoglycan layers. A study by Thomashow and Rittenberg concluded that glycanase, which is active only during penetration, begins to create a pore in the cell wall and peptidoglycan layer through which the bdellovibrio can enter the prey cell (11). They showed that the amount of peptidoglycan cleaved by the glycanase is also roughly the amount needed for the bdellovibrio to fit through if it were to enter the prey and advocated that this enzyme is solely responsible for creating the pore. However, the pore is created by the mechanics of the bdellovibrio pushing against its prey (12). A more recent study demonstrated that glycanase can not be solely responsible for creating the pore; Tudor *et al.* showed that in heat killed *E. coli* cells bdellovibrio can still penetrate the cell without release of solubilized glucosamine which is indicative of glycanase activity. Also, in a glycanase-defective mutant bdellovibrio strain, strain W, the prey cell can still be penetrated but it remains in its pre-penetration shape. Therefore it is most likely that the glycanase accounts for the rounded shape of the bdelloplast. It

is believed that a peptidase, present in all bdellovibrio strains, also contributes to the expansion of the bdelloplast, which occurs whether the bdelloplast is round or not.

Not only physical but also metabolic changes occur in the prey cell upon penetration by the bdellovibrio. First, the permeability of the prey outer membrane changes rapidly to release certain small molecules including lactose, acetate, and succinate. There is also a rapid decrease in the penetrated prey's respiratory potential as measured by the concentrations of several different end products of various metabolic pathways. This decrease in respiratory potential is indicative of a general disruption of a pathway common to all metabolic processes that occur in the cell and leads to the eventual death of the prey cell (13).

After outer membrane penetration, the bdellovibrio then makes its way entirely into the periplasmic space, losing its flagellum and not greatly disrupting the cytoplasm. This "bdelloplast", once formed, has a more hydrophilic nature than the prey cell had before the bdellovibrio entered the periplasmic space (14). The entire process of the entrance into the prey cell has been well characterized using electron microscopy (6, 7, 9). From this position, the bdellovibrio consumes the nutrients present in the invaded cell. As the bdellovibrio digests its prey, it lengthens in proportion to the size of the prey bacterium and eventually divides simultaneously into multiple new

progeny bacteria. These develop flagella and burst out of the prey bacterium (10).

It has been shown with SDS-PAGE, isoelectric focusing, and 2D gel electrophoresis that the bdellovibrio may place a protein in the cytoplasmic membrane of the prey cell (15, 16). This protein is thought to be a porin protein and similar in size to an *E. coli* OmpF protein or a bdellovibrio OMP. The action of placing a porin in the cytoplasmic membrane may be partly responsible for the almost immediate cell death due to the loss of membrane polarization seen after penetration.

There is evidence the bdellovibrio reuse various biomolecules from their prey cells, either in pieces or the whole molecule. Bdellovibrio are known to reuse nucleoside monophosphates from their prey's RNA (17). They may also take up outer membrane proteins (OMPs) from the prey cell, including OmpC and OmpF (16). However, this topic is very controversial as there are studies that have shown that bdellovibrios may produce their own porin and do not reuse porins from the prey cell (18, 19). The ability to take up OMPs is very strain specific. Strain 109J(1977), which had been in a lyophilized state for nine years until these outer membrane studies were performed, does take up OMPs, while strain 109J, continuously cultured in lab during those years, has a diminished capacity to take up OMPs. Strain 109J must have lost that ability during its years being actively cultivated in a

laboratory (20). Interestingly, membrane-derived oligosaccharides are thought not to be used by growing bdellovibrio (21).

There is still some debate as to whether bdellovibrio incorporates whole LPS of their prey into their outer membrane. It is a hard question to answer with current techniques as there is no way to remove all prey cells from a suspension of bdellovibrio. Nelson and Rittenberg concluded that there were two fractions of LPS isolated from *Bdellovibrio bacteriovorus* 109J, one unique to the bdellovibrio and one similar to that of the *E. coli* prey in thin-layer chromatography analysis (22). They also determined that the bdellovibrio obtained portions of their fatty acids and amino sugar from their prey cells (23). Bdellovibrio does have a system in place that allows for modification of fatty acids that may have been obtained from its prey (24). Most recently, a German group analyzed both fractions and discovered a distinct difference in the lipid A head group between both the LPS fraction unique to the bdellovibrio and the LPS fraction equivalent to that of the prey as well as the prey LPS itself. The bdellovibrio LPS contains neutral mannose sugar groups in place of the phosphate groups found in the *E. coli* LPS isolated from prey cells (25). Thus, it is possible that bdellovibrios take up prey LPS but modify it before use and place distinctive LPS on their cell surfaces.

## Section 2: The Gram-Negative Cell Wall

The Gram-negative cell wall is a remarkable structure. It is responsible for the ability of Gram-negative bacteria to survive changes in pH and temperature. The makeup of the cell wall follows a general pattern and is very similar over many species of Gram-negative bacteria, especially when compared to Gram-positive cells, whose membrane composition can vary greatly between species. The Gram-negative cell wall is composed of an outer membrane around a peptidoglycan layer, both surrounding an inner cell plasma membrane. The outer membrane and the plasma membrane sandwich the periplasm, filled with a gel-like matrix called the peptidoglycan (Fig. 2) (26).

The outer membrane is composed of proteins, phospholipids, and lipopolysaccharides (LPS). The lipids are distributed asymmetrically between the inner and outer leaflet. The inner face is composed mostly of phospholipids, whereas the outer face contains almost all of the LPS in the cell. This distribution makes the outer membrane of a typical *E. coli* cell anionic at neutral pH, since the lipid A, cores, and O-antigens (if present) of LPS contain exposed phosphoryl and/or carboxyl groups that can interact with cations in the environment. The outer membrane may contain more than one type of LPS (26).

LPS is made of four main components (Fig. 3). The first, and incidentally most essential part for bacterial virulence, is the lipid A moiety.

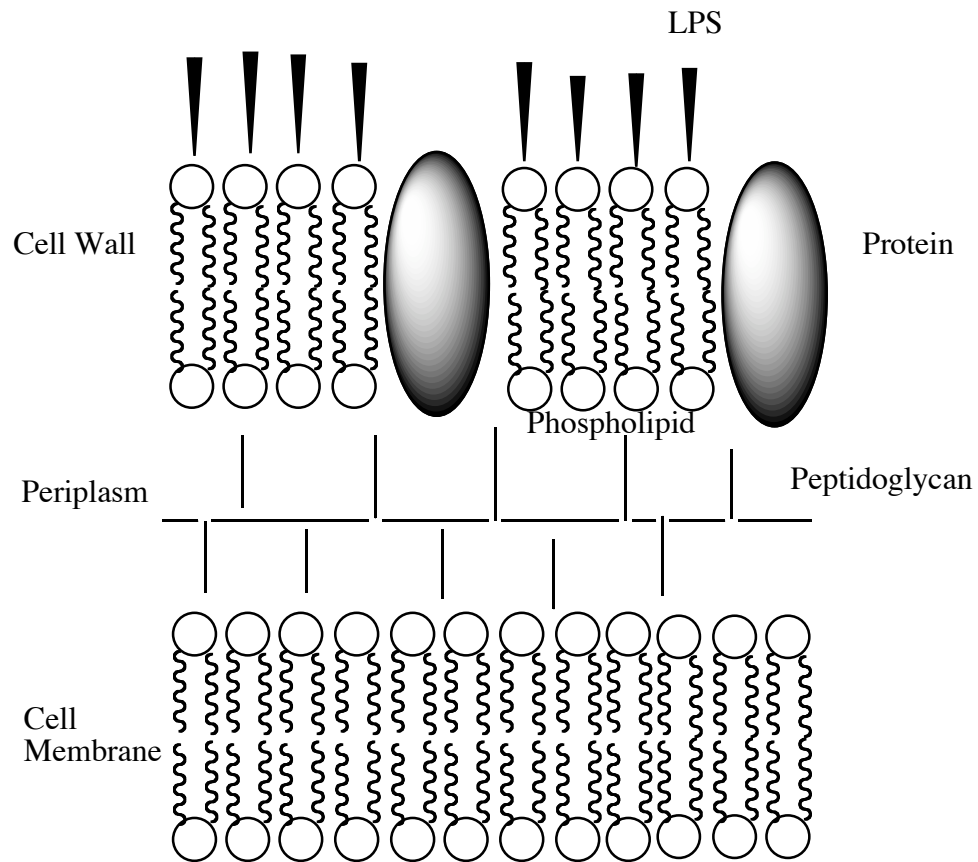


Figure 2: Diagram of the Gram-negative bacterium cell wall. The cell wall is depicted as the outermost layer made of two leaflets. The outer leaflet is composed of LPS molecules while the inner leaflet is composed of phospholipids. There are also proteins that span the cell wall. Underneath the cell wall is the periplasm. The periplasm contains the peptidoglycan, shown here as a network of interconnected lines. The last layer is the cell membrane, made up of lipids.

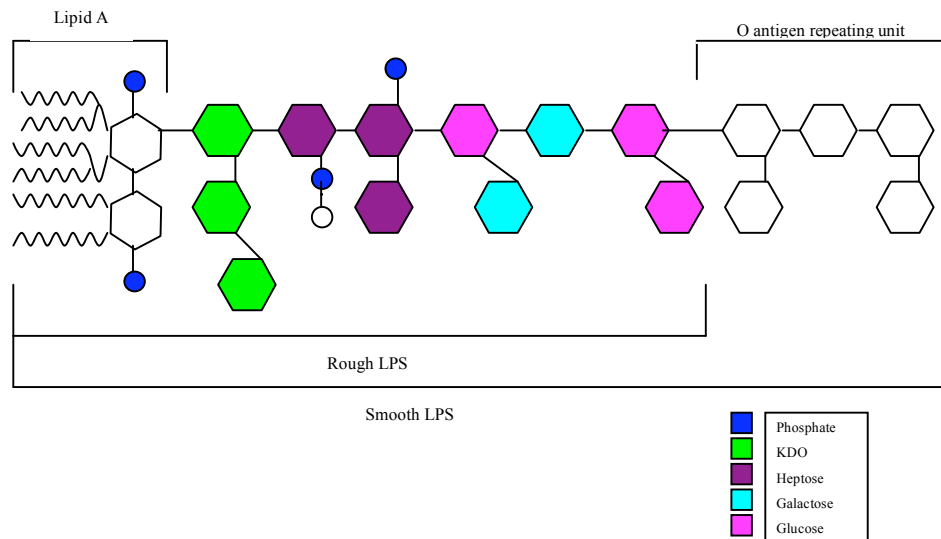


Figure 3: Schematic drawing of a generic *E. coli* type LPS molecule. The lipid A is composed of phosphorylated glucosamine with fatty acid tails. Note the phosphate groups attached to the lipid A head. There are usually 20 to 40 O antigen repeating units in one LPS molecule. This schematic drawing is of a typical *E. coli* LPS molecule (27).

The lipid A is made of six or more fatty acid chains that are linked to two phosphorylated glucosamine molecules. In typical *E. coli* strains, four of these fatty acids contain hydroxyl groups while the other two do not. The lipid A can be a source of variation within the LPS molecule. The lipid A can differ in several ways: in the number of fatty acids and the length of the fatty acid residues, since typically three or four different fatty acids are present with lengths between 10 and 16 carbon atoms, in its acylation, which can be either symmetric or asymmetric; and the presence of 4-amino-deoxy-L-arabinose and/or phosphoethanolamine attached to the glucosamine sugars. These variations can occur between strains, species, and genera, but *E. coli* strains tend to follow a similar pattern.

The inner core and outer core make up the second and third sections of the LPS molecule. The inner core usually consists of two or more 2-keto-3-deoxyoctonic acid (KDO) molecules. These molecules are linked to the glucosamine of the lipid A head. Two or three L-glycero-D-manno-heptose sugars are attached to the KDO to complete the inner core. The outer core has a more variable sugar composition than the inner core, but it is composed of more common sugars such as glucose and galactose.

The outermost part of the LPS is the O-antigen that is attached to the terminal sugar of the outer core. The O-antigen extends from the core, and like the lipid A moiety, is highly immunogenic. There is huge interspecies and interstrain variation in the O-antigen. It is composed of repeating units of

common sugars. Each unit is composed of three sugars, with an extra sugar attached to the first and third sugar. Anywhere from 0 to 40 units compose the O-antigen. Molecules that contain an O-antigen are labeled smooth bacterial strains (27). Smooth strains tend to have a higher degree of heterogeneity in their composition and may contain LPS molecules with differing numbers of O-antigen repeating units (28). Bacteria whose LPS lack the O-antigen are labeled rough strains (27). Rough strains, so named because the bacteria have rough appearance, have more homogenous LPS (28).

The LPS of bdellovibrio strains HD100 and HI100 (a host independent strain) has been analyzed by various chemical and immunological methods, giving us a good starting point for the analysis of 109J. Schwudke *et al.* determined that the HD100 and HI100 contained  $\alpha$ -D-mannoses in place of the charged phosphate groups present in the lipid A head groups found in the LPS of the prey cells (25). This group used mass spectrometry, nuclear magnetic resonance (NMR) spectroscopy, and murine monoclonal antibodies to characterize the different parts of the lipid A and concluded that there was a significant difference in the head group of the LPS of the bdellovibrio and that of its prey, *E. coli* strain K12. They separated bdellovibrio LPS from the less soluble prey-derived LPS. They noticed that the LPS of HI100 precipitated from the solution of isolated LPS in ethanol and used this to obtain bdellovibrio LPS. The structure of the LPS from this bdellovibrio strain is shown in Figure 4. If the same substitution of neutral for charged molecule in

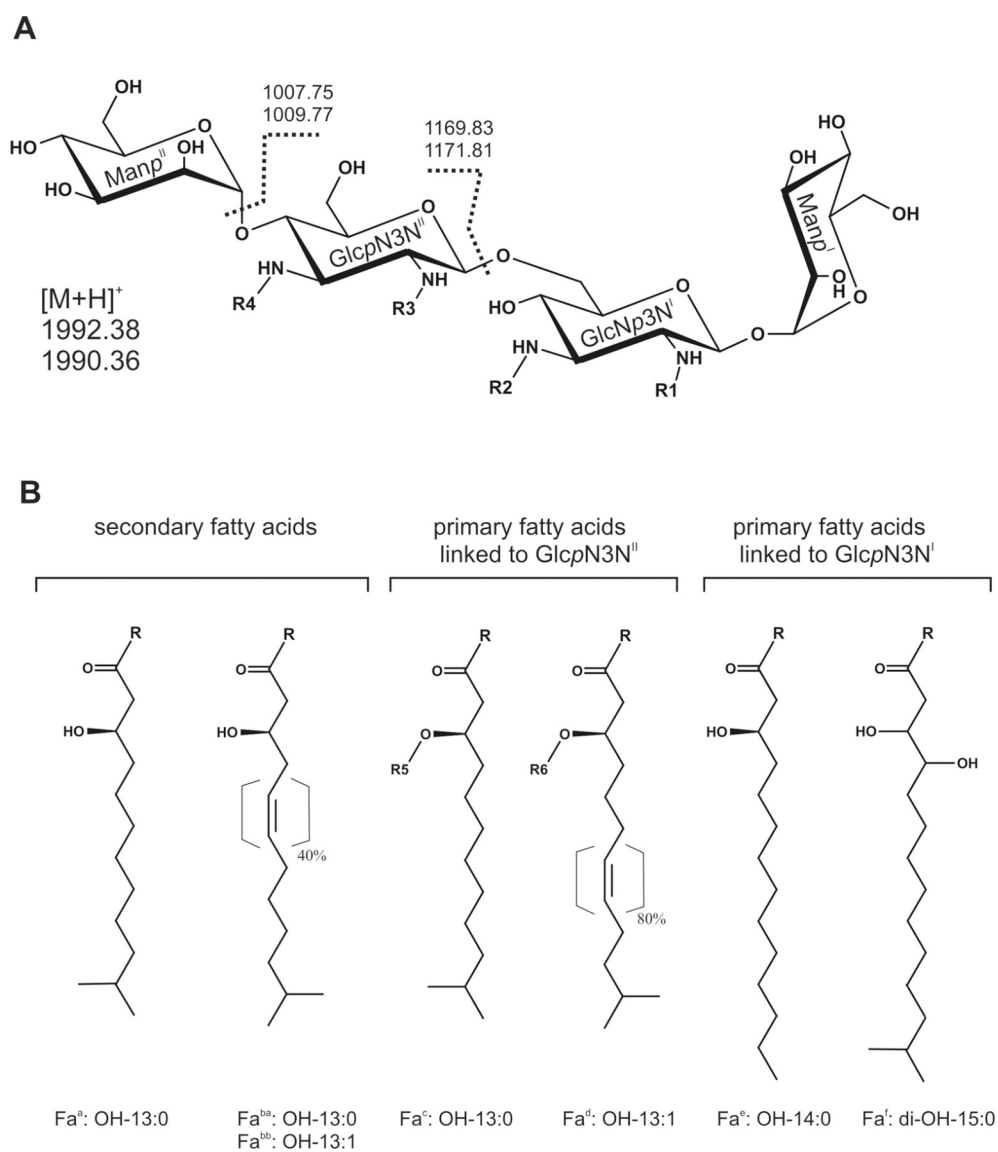


Figure 4: The structure of the LPS of the *Bdellovibrio bacteriovorus* HD100 as determined by Schwudke *et al* (25). Part A shows the lipid A head group. There are two mannose sugars in the lipid A head group in the place of the phosphate groups that are seen in Figure 2. In part B, the fatty acid tails are shown. This image is from the work by Schwudke *et al*.

the lipid A head holds true in bdellovibrio 109J, it might be involved in prey recognition in all strains of bdellovibrio.

The bdellovibrio prey *E. coli* K12 strain W3100, a rough strain, has well-characterized LPS. Two analyses were completed by the same group using the same methods. In their first paper on the topic, the group used electrospray ionization-Fourier transform ion cyclotron-mass spectrometry (ESI-FT-MS), NMR, and gas liquid chromatography to look at LPS (29). They reported that this strain of *E. coli* had sugars Rha, Glc, Hep, Kdo, GlcN and phosphate in the molar ratio of 0.2:2.8:1.0:4.1:1.9:2.1:5.1. The fatty acids of the lipid A were determined to contain 3-OH-C14:0 tetradecanoic acid and dodecanoic fatty acids, which are the same acylation patterns as seen in other *E. coli* strains. Eleven molecular species were present along with four different glycoforms. In the second study, two other members of the group used various mass spectrometric methods to determine the structure of both the K12 W3100 and another *E. coli* strain (Fig. 5) (30).

Another group in France used similar methods to study the lipid A of *E. coli* strain O111:B4 along with other *E. coli* and *Salmonella* LPS and synthetic lipid A molecules (31). Using plasma desorption mass spectrometry, they found that the fatty acids of the O111:B4 lipid A were composed of a predominantly hexa-acyl species, with penta- and tetra-acyl species appearing in small amounts. They concluded that the lipid A was similar to a synthetic *E. coli* type lipid A. The lipid A head was typical of

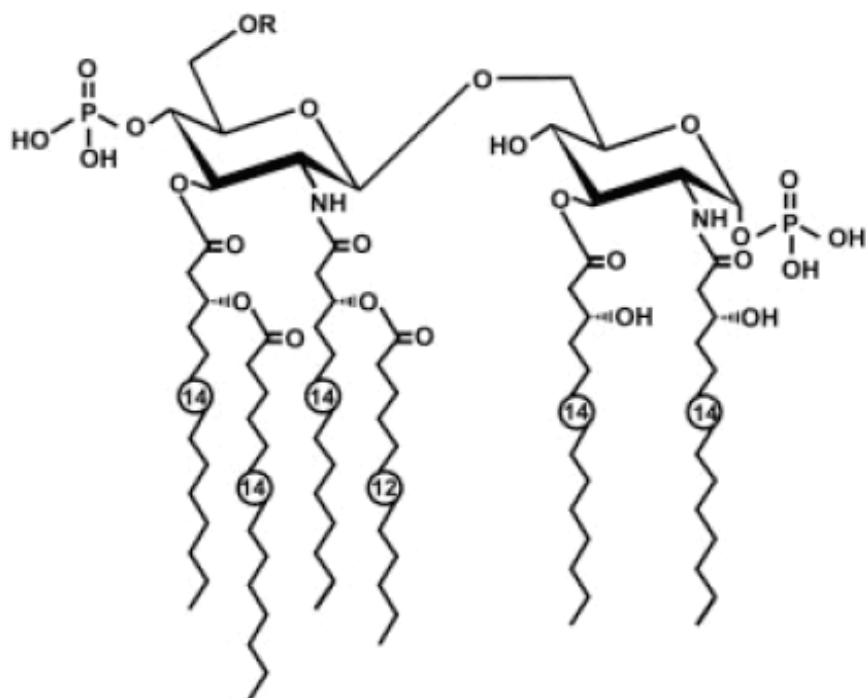


Figure 5: A drawing of the LPS molecule isolated from the *E. coli* K12 strain W3100. This image was taken from the work by Muller-Loennies *et al.* (29).

those found in other *E. coli* species. Thus the O111:B4 LPS structure (Fig. 3) can also be compared to that of bdellovibrio.

### **Section 3: Purpose**

*Bdellovibrio* presents a unique question for study: how is it that the bdellovibrio preys only on Gram-negative bacteria but it itself is Gram-negative and does not attack other bdellovibrio? Bdellovibrios must identify some recognition molecule, structure, or physical property in the cell wall of Gram-negative bacteria to determine whether the bacterium is a suitable prey cell or not. It must be a molecule in the cell wall; bdellovibrio binds reversibly to a variety of cells and non-cell surfaces before penetration and, as stated above, bdellovibrio shows no chemotaxis toward its prey. The bdellovibrio is not a sophisticated hunter. It is observed hunting in suspension where it indiscriminately swims into other cells. This recognition molecule is most likely not a protein because a protein could mutate quickly, making prey cells immune to bdellovibrios, a process which is not seen. Most likely, bdellovibrio recognizes some part of the LPS molecule because of its considerable presence in the outer membrane. In this work, various chemical and biological techniques will be used to characterize LPS from several different *E. coli* strains and bdellovibrio to determine if there is a difference in their structure or in the membranes they make. Once characterized, bdellovibrio that express the GFP gene will be exposed to LPS monolayers

and their binding affinity will be quantified. If bdellovibrio have a high binding affinity for LPS from the *E. coli* and no binding affinity for the LPS from the bdellovibrio, there is strong support for LPS being the recognition molecule.

#### **Section 4: Supported Lipid Membranes**

A supported lipid membrane is a layer of lipids that is held up by some sort of solid substrate. It can either be a monolayer, a bilayer, or have many layers, depending on how many layers are deposited (32). Supported lipid layers are an extremely useful tool for studying the physical properties of membranes as well as cellular interactions. Because of the commercial availability of many different cellular components as well as the ability to extract exact cellular components, we can prepare model cell surfaces to determine the minimal requirements for recognition. In addition to a variety of phospholipids and LPS, specific proteins and cholesterol can be included within these uniquely created bilayers (33).

The pioneering work on monolayer deposition was performed by Irving Langmuir in 1917 (34). He worked on spreading films made of oil onto water until the oil had no more tendency to spread. The layer was contained and manipulated by barriers that were part of a self-designed trough which he used to place these layers on a substrate; adjusting the barrier position lead to a change in the molecular packing density of the oil. He also

examined the chemistry behind the interaction of oleic acid and water, concluding that the carboxyl group interacts with the water but the hydrocarbon chains interact with each other, thus forming a movable layer. This was one of the first studies to critically analyze amphipathic molecules. He also explored the compressibility of the monolayers and the interactions of the molecules. Katherine Blodgett expanded on this work in 1935 using layers of calcium stearate which she deposited in successive monolayers from a water layer on to a glass slide. She modified Langmuir's original trough to suit this purpose (35).

The first step in creating a supported lipid bilayer is to establish the support. The bilayers that are created must somehow be affixed to the substrate on which they are created or it would be difficult to effectively utilize them. There are several ways to create this support. The first way to adhere a lipid bilayer is by fixing the bilayer to the substrate covalently or through ion bridges. The second possibility is to freely support a lipid bilayer with a thin film of water. The third method is to create a bilayer on a soft polymer film. Lastly, a layer of alkylsilane can be deposited on the surface to support the monolayer (32).

The simplest way to create supported lipid bilayers is to employ a Langmuir-Blodgett trough as illustrated by Blodgett (35). Using a modern Langmuir-Blodgett trough, a relatively simple apparatus composed of a contained, air-water interface, a well through which the support can be

lowered or raised through the interface, and a computerized lever that can alter the density of the lipid layer, it is possible to create highly specific lipid layers that can be attached to a surface, usually glass, mica or single crystal silicon. To create a supported lipid bilayer useful for experiments involving cellular membranes, a hydrophilic substrate is raised through a monolayer made up of the molecules that would characterize the inner leaflet of the membrane. Then the same slide is dropped slowly through another monolayer, this time composed of the molecules that make up the outer leaflet of the membrane. The main benefit of this technique is that both layers of the bilayer can be manipulated (33). This technique can also be used to create a supported monolayer if only one layer is deposited. It can be used to create monolayers with the lipid tails facing either out into the environment or in to the substrate (Fig. 6).

Another way to create supported lipid bilayers when the specificity of the inner leaflet of the membrane is not important is by a method called vesicle spreading. This method was first set out by Brian and McConnell in their studies of cytotoxic T cells (36). First a glass cover slip is cleaned with an argon spray and then made hydrophobic with octadecyltrichlorosilane. Then the cover slip is placed on top of a solution of phospholipid vesicles, in their case egg phosphatidyl choline (PC) and cholesterol, resulting in a uniform bilayer formed over the glass. This method is not useful for creating

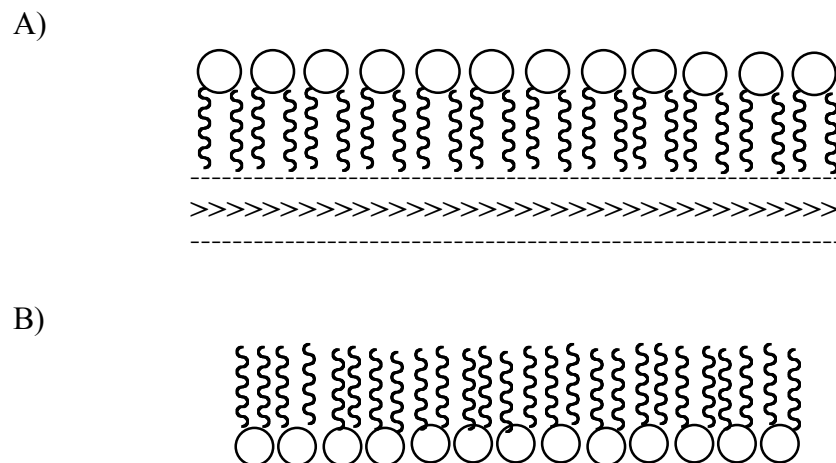


Figure 6: Schematic supported lipid monolayers. These schematic diagrams represent the two types of monolayers that were formed in this work. A) Image A is a schematic drawing of a lipid monolayer formed by hydrophobic interactions with the head group facing out. The tails are aligned with a layer of alkylsilane molecules, represented by the arrow heads, which are attached to a glass slide. B) Image B is a schematic drawing of a lipid monolayer formed by electrostatic interactions on mica with the tails facing out. The head groups are touching the mica.

monolayers, as the lipids are more likely to interact with themselves to form multiple layers on the support.

Once the supported bilayers are created, it is possible to image them using atomic force microscopy (AFM) (Fig. 7). This technique allows the observer to determine whether or not the bilayer has formed correctly on the substrate or whether there were poor interactions between the monolayers and the substrate resulting in large holes in the membrane produced (37). A good review of AFM use in various supported membranes is found in Rinia and de Kruijff (38). Many monolayers are observed in fluid, with the tails facing down on to the support.

Sometimes it is useful to place the molecules in the opposite orientation with the tails facing into air. The stronger electrostatic interactions between the substrate and lipid stabilize the monolayer; in liquid the individual molecules are very fluid. Roes *et al.* found that in a monolayer made from LPS of an *E. coli* rough mutant there appeared to be domains forming within the monolayer of a higher compression than that of the surrounding monolayer (39).

Based on these previous works, we made two types of supported LPS monolayers of the LPS of *Bdellovibrio* and several prey strains, both rough and smooth. We analyzed these monolayers using AFM and found that the LPS monolayers formed on the alkylated cover slips were all very similar,

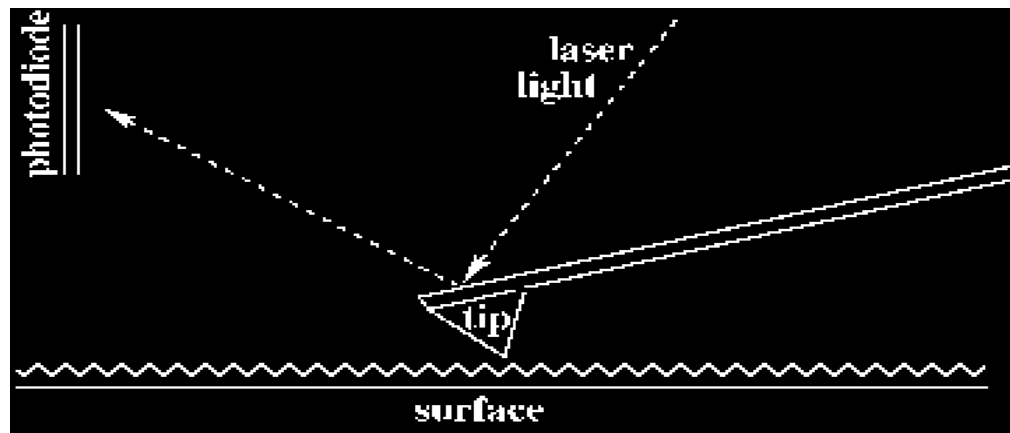


Figure 7: A schematic drawing displaying the basic functioning of an Atomic Force Microscope (AFM). In AFM a laser shines onto the tip. As the tip moves over the surface, changes in the deflection of the laser on the tip are registered on the photodiode. These changes are interpreted by a computer to generate an image.

regardless of the designation of the LPS. When monolayers were formed on mica, the rough LPS formed very different monolayers than the smooth LPS.

## CHAPTER 2: MATERIALS AND METHODS

### Section 1: Growth and Characterization of *Bdellovibrio*

*Bdellovibrio bacteriovorus* 109J was purchased from American Type Culture Center (Bethesda, MD) and revived in 25 mL of a HEPES/metals (HM) solution consisting of 10 mL of a 1M HEPES buffer at pH 7.6 and 1 mL of a 1M CaCl<sub>2</sub> and 0.1M MgCl<sub>2</sub> (metals) solution per liter. The final concentration of this solution was a 10 mM HEPES, 1 mM CaCl<sub>2</sub>, and 0.1 mM of MgCl<sub>2</sub>. This culture was incubated overnight at 30°C before 10 mL of the bdellovibrio suspension was added to three different flasks each containing 50 mL of HM and 10 mL of *E. coli* grown in Difco Nutrient Broth (NB). A control culture containing just *E. coli* was also used as a comparison to monitor the clearing of prey from the suspension. These culture conditions were used only to revive the bdellovibrio.

To grow an active bdellovibrio culture, 5 mL of an *E. coli* culture grown in Difco Nutrient Broth (8 g Difco nutrient broth, 1 g yeast extract, 5 g casamino acids per liter) was added to 45 mL of HM in a 500 mL Erlenmeyer flask, making a 10% Dilute Nutrient Broth (DNB). The scale of the culture could be increased if a larger amount of bdellovibrio was desired as long as the suspension occupied equal to or less than 10% of the flask volume. The

suspension of bdellovibrios and *E. coli* were allowed to grow in a 30°C shaking incubator for three to five days. The cells were then observed under a light microscope to determine if the bacteria were alive and active. The bdellovibrio were observed to have a distinctive motility from the movement of the *E. coli* cells and were much smaller than the prey cells.

The bacteria were then imaged using AFM to observe the bdellovibrio growing inside its prey. Samples were prepared by placing 10 µL of either a bdellovibrio culture or a control culture on to a sterile 0.45 µm filter on a DNB plate and allowing it to sit at 30°C overnight (40).

Bdellovibrio and *E. coli* strains were frozen at -80°C for storage. The bdellovibrios were frozen with prey cells in glycerol (2) or in dimethyl sulfoxide (DMSO). Bdellovibrios were grown in DNB and *E. coli* suspension and, after 24 hours, 1 mL of that solution was added to either 0.5 mL of sterile 50% glycerol or 1 mL 10% DMSO. The ML35 was frozen with the same glycerol method used with the bdellovibrios. Both bacteria revived well from their frozen states.

## **Section 2: Prey Cell Selection**

For final prey cell selection two criteria were used. The chosen strains were either commonly used as bdellovibrio prey or had well characterized LPS. *E. coli* strains ZK1056 and ML35 were chosen because of their previous use as prey cells, O111:B4 was chosen because it has well characterized LPS,

and K12 W3100 was chosen both because it is good prey and has well characterized LPS.

Cell counts were performed to quantify bdellovibrio's preference for the O111:B4, the only prey strain that had not been used previously. At the same time, K12 was also used for cell counts to provide a comparison. Serial dilutions were plated throughout a growth cycle for four days. Both suspensions growing bdellovibrio on prey and suspensions that simply contained the prey in DNB were measured. Each suspension was set the same as a typical bdellovibrio growth cycle; 5 mL of the appropriate prey was added to 45 mL of HM and inoculated with 1 mL of bdellovibrio and grown at 30°C. Once it was available, the bdellovibrio used was that from the previous growth cycle in each specific prey. Every 24 hours, over 4 days, 0.1 mL of suspensions of  $10^{-5}$  to  $10^{-9}$  were plated on LB plates and allowed to grow overnight at 37°C. By plating on LB and growing at 37°C, any bdellovibrio would be killed and would not skew the counts. The colonies that had grown on the plates were counted and used to determine the number of cells per mL in each suspension. The log of that number was graphed and for each strain, the suspension with bdellovibrio was compared to that without.

### **Section 3: LPS Extraction**

To begin the LPS extraction process for the *E. coli* strain ML35, two liters of NB were inoculated with ML35 and grown overnight. The cells were

centrifuged at 2700 xg at 4°C for 15 minutes. The supernatant was discarded and the cells lyophilized.

The hot phenol-water method of Westphal and Jann was utilized to isolate the LPS (41). During each extraction step and the dialysis, 0.6 mL of the water layer was removed. During each centrifugation step, 0.6 mL samples were collected from the supernatant and the resuspended pellet. These samples were placed into a 1.5 mL epindorf tube for further characterization. Using approximately 0.5 g of dried bacteria, 8.75 mL of 65°C phenol and 8.75 mL of 65°C distilled water were mixed in a Nalgene capped centrifuge tube. The mixture was heated and stirred in a 65°C water bath for ten minutes. It was then cooled in an ice bath and centrifuged at 3000 rpm for 45 minutes producing 3 layers. The aqueous layer was least dense, underneath which was a layer of insoluble cellular material, with the phenol layer on the bottom. The water layer was removed and retained. The phenol layer is extracted twice more with 8.75 mL of hot, distilled water. The LPS and nucleic acids remained in the aqueous layer and most of the proteins and phospholipids remained in the phenol layer and interface.

Once all three extractions were combined, they were dialyzed against water at 4°C for 3 days. This process removes any phenol that might have accidentally been removed with the water layer. The solution appeared slightly opalescent, just as described in the literature (41).

The dialyzed extract was centrifuged in a Beckman centrifuge at 10°C for 10 minutes at 3000 rpm. The pellet, containing any remaining insoluble material, was discarded. The supernatant was collected and lyophilized in a process that took approximately 2 days. The solid, generally about 0.15 g, was dissolved in about 30 ml of distilled water. This solution is centrifuged overnight at 10,000 rpm. The supernatant was saved to determine if there were any LPS present. Once it was determined that there was only a small amount of LPS, the supernatants were discarded. The resuspended pellet was centrifuged twice more at 10,000 rpm for overnight using the same procedure.

After centrifuging was complete the pellet was suspended in a small amount of water and lyophilized again. Once the lyophilization was finished, the LPS were weighed. The isolated lipids were then resuspended in chloroform to make a 1 mg/mL solution and stored in a -20°C freezer.

Based on the results obtained from the ML35 extractions, it was decided that the lyophilized bacteria only needed to be extracted twice; the third extraction did not greatly increase the amount of LPS in the final solution but did appear to increase the amount of protein and DNA that was present. The third centrifugation of the final centrifugation step was also deemed unnecessary and was omitted from later LPS isolations.

A unique problem presented itself with the bdellovibrio. Since the bdellovibrio are grown on another bacterium, the cultures contain cell debris that must be removed to eliminate any contaminating LPS. In order to

separate the bdellovibrio from prey cells and cell debris for LPS isolation, differential centrifugation was used. Because the bdellovibrio is so much smaller than its prey, an initial centrifugation was performed at 700 xg for 15 minutes. The bdellovibrio remained in the supernatant while the ML35 (the prey for the bdellovibrio for this isolation) pelleted out. The supernatant was then centrifuged again at 10,000 xg for 15 minutes, this time pelleting out the bdellovibrio and leaving most of the cellular debris from the prey in solution. These centrifugations allowed the contamination from the ML35 LPS to be kept to a minimum.

#### **Section 4: SDS-PAGE and Agarose Gel Electrophoresis**

Several types of electrophoresis and staining techniques were used to determine what molecules were present in various stages of the extraction process. For each aliquot taken from the extraction, a sample was prepared to detect for proteins, LPS, or nucleic acids.

First, two polyacrylamide gels were run containing identical samples. The gels were run following the procedure of Laemmli (42), with a 3% stacking gel and a 14% separating gel as recommended by Tsai and Frasch (43). The samples were prepared by combining 10  $\mu$ L of the aliquot with 10  $\mu$ L of a loading buffer composed of 2% SDS, 20% sucrose, 1% 2-mercaptoethanol, and 0.001% bromophenol blue. A DNA standard (Bio-Rad) and low molecular weight protein standard (Bio-Rad) were prepared

containing 1  $\mu\text{L}$  of the standard solution and 10  $\mu\text{L}$  of the loading buffer. During preliminary runs, the loading buffer was not visible once the samples began to run through the gel, so 1  $\mu\text{L}$  of a 6X glycerol based running dye was added to each sample. O111:B4 LPS from Sigma was used as the LPS standard. 5  $\mu\text{L}$  of the chloroform solution was dried down with nitrogen gas and reconstituted in distilled water. It was then prepared in the same manner at the other samples. The samples were then heated at 100° C for five minutes. 20  $\mu\text{L}$  of the heated sample was loaded in to the wells. The gels were then electrophoresed for one to two hours at 40 mA.

One of the gels was then stained with a Coomassie Brilliant Blue stain for four hours to detect any proteins. It was then destained in a 40% methanol and 5% acetic acid solution. The solution was switched over after one hour and then left to destain overnight. The gel was then photographed on a light box. Any protein appeared as blue bands (44).

The second gel was stained for LPS using a silver staining technique adapted from a protein staining technique presented by Tsai and Frasch (43). First the gel was fixed overnight in a solution of 40% ethanol and 5% acetic acid. It was then oxidized in the fixing solution mixed with 0.7% periodic acid for 10 minutes. Then the gel was washed three times with water for 15 minutes each. After washing, the gel was stained with a freshly prepared silver stain, composed of 1 mL ammonium hydroxide, 1.4 mL 1M sodium hydroxide, 2.5 mL 20% silver nitrate solution, and 70.1 mL distilled water.

The gel was submerged in the staining solution for 10 minutes and then washed three times for 10 minutes each. The gel was then developed in a formaldehyde and citric acid developer. The LPS was stained brown, sometimes quickly, to the point that the background was also stained brown and the bands were only visible on a light box. Sometimes this process occurred very slowly, taking a day to fully develop. Once the gel was done developing, it was photographed in the same manner as the protein gel.

An agarose gel was also run to determine the DNA content at each step. A 1% agarose gel was run at 100 volts with the same samples as the polyacrylamide gels. The samples were prepared for loading by adding 5  $\mu\text{L}$  of the sample to 3  $\mu\text{L}$  of 6X running dye and 12  $\mu\text{L}$  of 1X TBE. The standards were prepared the same way, except the LPS had to be dried and reconstituted in water and only 1  $\mu\text{L}$  of the DNA and low molecular weight protein standards were used. After the gel was finished, it was photographed on a UV light box. Polyacrylamide and agarose gels were also run to assess the purity of the extraction process for both the ZK1056, *bdellovibrio*, O111:B4, and K12 LPS. They were run in the same manner as the gels described above.

### **Section 5: Formation of supported lipid membranes**

In creating supported lipid monolayers, the first step is to obtain clean glass cover slips by washing in a solution of sulfuric acid and Nochromix.

This somewhat harsh oxidation removes any oil and dirt and makes the cover slip hydrophilic. The cover slip is then placed into an air free container with 0.5 mL of an octotriethoxysilane compound (Sigma) and heated to approximately 60°C overnight. Heating allows the compound to attach to the cleaned glass cover slips in an even manner, making it hydrophobic. The contact angle, the angle a drop of water makes with a surface, was measured between 90 and 110 degrees.

Once the glass was made hydrophobic it was possible to form a model membrane on it. A mixture of 50  $\mu\text{L}$  of fluorescently labeled phosphatidyl choline (PC) and 500  $\mu\text{L}$  unlabeled PC were used for initial characterizations; later pure LPS solutions were used to form monolayers. A 50  $\mu\text{L}$  sample of the LPS solution, still in chloroform, was placed on the surface of a Petri dish filled with distilled water. Once the chloroform had evaporated an alkylated glass slide was slowly pushed through the LPS layer into the water. If the supported monolayer was to be imaged by AFM, the cover slip was left in the water, and adhered to the Petri dish with double sided tape. Excess LPS were washed from the monolayer by swirling the contents of the Petri dish without exposing the monolayer to air. Any excess LPS molecules were then vacuumed from the surface with an aspirator. A layer of water was left covering the cover slip to keep the monolayer intact.

Reverse monolayers were also created when a hydrophilic, freshly cleaved piece of mica was placed in a Petri dish filled with distilled water. A

layer of LPS was placed on top of the distilled water in the same manner as before. The mica was then pulled up through the LPS and super-glued onto a metal AFM disk (Ted Pella). Because the mica is negatively charged, the LPS molecules orient themselves with the tails of the lipid A moiety facing the air. The monolayer was allowed to dry and was then imaged in the air in contact mode.

FITC labeled O111:B4 LPS and unlabeled LPS from Sigma were then used for normal, “tail down”, AFM monolayers and fluorescence microscopy. The fluorescent and the non-fluorescent component of the LPS solutions were mixed in a 1:10 ratio, dried with nitrogen, and then resuspended in water. The solutions were bath-sonicated to ensure complete mixing. This solution was then applied to the hydrophobic glass in the same way as the PC, and observed using AFM. These solutions were also used to create layers held between the cover slip and a slide to observe using fluorescent microscopy to determine the overall coverage of the slide.

LPS monolayers were also constructed from the extracted ML35 LPS, ZK1056 LPS, *bdellovibrio* LPS, O111:B4 LPS and K12 LPS, as well as the purchased samples of *P. aeruginosa* LPS, EH100 LPS, and O111:B4 LPS. Since there were no fluorescently labeled LPS for any of the strains commercially available besides the O111:B4, similar coverage studies could not be undertaken with the fluorescent microscope.

## Section 6: AFM Observation

After the monolayers were formed, they were characterized using AFM (Dimension 5000, Veeco/Digital Technologies). Most scans were done over a 5 micron by 5 micron area but larger scans were also used especially if an area was being scratched. The scanning speed was kept at 0.5 Hertz and the scan size was 256 pixels by 256 pixels. For a scan of 5 by 5 microns, it took approximately 10 minutes to complete one scan. The tip used was an oxide-sharpened silicon contact tip (Veeco). All scans were taken in the contact mode, both height and deflection images were captured. Since some of the images were taken under fluid, a water-proof tip holder was used.

First, cleaned glass and alkylated glass were observed. Clean glass was attached to a Petri dish using double sided tape and the Petri dish was filled with distilled water. The entire Petri dish was then placed under the scanner. Since the alkylated glass was so hydrophobic, it was not possible to image it underwater and so it was glued on a metal disk (Ted Pella), positioned directly under the tip, and imaged in air. The freshly cleaved mica was imaged in the same way as the alkylated glass.

The LPS monolayers were observed under distilled water in contact mode using the same protocol as described above for the cleaned glass. Imaging the monolayers under fluid allowed them to be kept in a more native form while they were imaged. The monolayers that were formed on mica with the tails facing out were imaged in air. The mica, once the monolayer

was deposited, was attached with superglue to a metal AFM disk. This was placed under the tip and imaged as before. Most images needed to be flattened before they could be interpreted; this was accomplished using the imaging software provided with the AFM.

## CHAPTER 3: RESULTS

### Section 1: Bdellovibrio characterization and predation of *E. coli* strains

#### O111:B4 and K12

As obligate predators, bdellovibrios must be grown and sustained on prey organisms. We initially prepared and characterized bdellovibrio with a common *E. coli* lab strain. Several techniques were used to monitor the bdellovibrio growth. Light microscopy (data not shown) was used to get a general idea of the health of the bdellovibrio culture. In a good culture the bdellovibrio could be seen swimming through the remaining prey cells. Over the course of several days of observation, the relative amount of prey would decrease while the relative amount of bdellovibrio would increase.

Next, AFM was used to look closely at the bdellovibrio growing inside its prey. As Figure 8 A shows, bdellovibrios were characterized in ML35 prey cells using contact AFM. There is a visible bdellovibrio inside a rounded bdelloplast near the center of the image, as indicated by the arrow. The bdellovibrio is most clearly visible in the deflection image seen on the right. The bdelloplast is approximately 1 micron in diameter. The bdellovibrio inside the bdelloplast is approximately 1.5 microns. It has curved around the side of the prey cell and curved in on itself. The bdelloplast can be contrasted

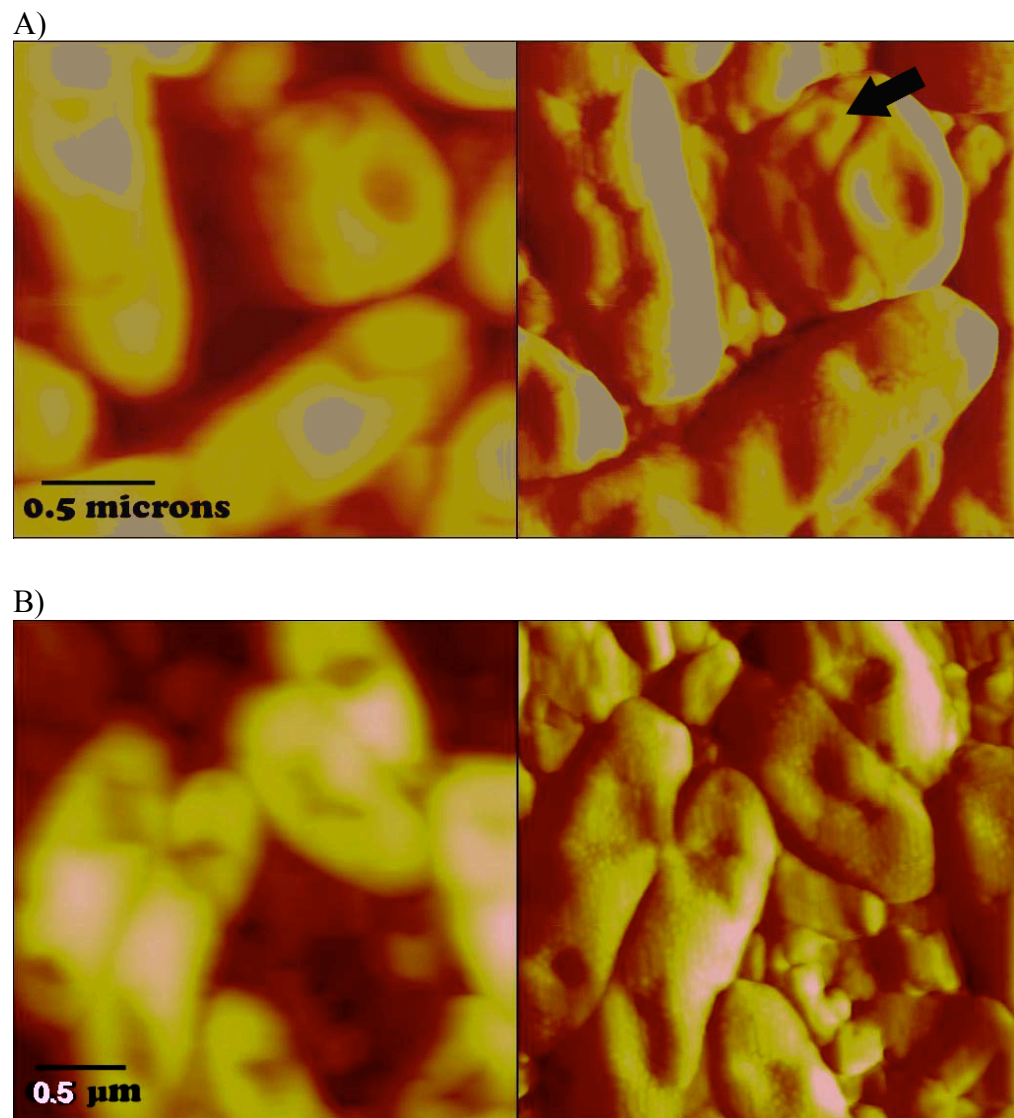


Figure 8: Bdellovibrio growing within a ML35 prey cell. A) The picture of a bdelloplast with a visible bdellovibrio inside in part A was taken with AFM in contact mode. The bdelloplast is about 1  $\mu\text{m}$  in width. The bdelloplasts were prepared by placing a suspension containing the prey cells on to a sterile filter on a DNB plate. A suspension of attack-phase bdellovibrios was placed on the filter as well. After 24 hours the filters were observed for bdelloplasts.

The image is 2.23 microns across and 2.23 microns tall. B) The second image shows only unattacked ML35 prey cells. The image is 2.84 microns across and 2.84 microns tall. The *E. coli* cells were approximately 2  $\mu\text{m}$  long.

with the two normal *E. coli* ML35 cell on either side as well as to the image of the ML35 control cells seen in Figure 8b. The *E. coli* cells in Figure 6a are approximately 2 microns long and 0.75 microns wide. The ML35 prey cells seen in Figure 8b are of similar size. These cells appear wrinkled as they were dehydrated from growing on a filter. The background of both images is filled with extracellular excretions and cellular debris.

Bdellovibrio predation was also monitored using a cellular counting technique to determine how well the bdellovibrio attacked the *E. coli* strains O111:B4 and K12. Each prey colony on a viable plate was counted and the number of colonies was used to determine the number of prey cells per mL of the culture. Figure 9a shows all of the calculated prey cell amounts for a four day O111:B4 growth period. Without considering whether or not bdellovibrio is present, it appears that the number of cells increases to day two and then decreases through day four. However, when trying to determine if there is a difference between the cultures grown with bdellovibrio present and those grown without, it is apparent that there is so much overlap in the number of cells that no difference can yet be elucidated. In the first three days all the data points had a great deal of overlap. Only two cell counts were obtained on day four, due to forces beyond our control. Figure 9b shows all the calculated cell amounts for a four day K12 growth period. It appears, when considering the data as a whole, there is a general increase in the number of cells per mL over each day. On each day, like the O111:B4 totals, the data

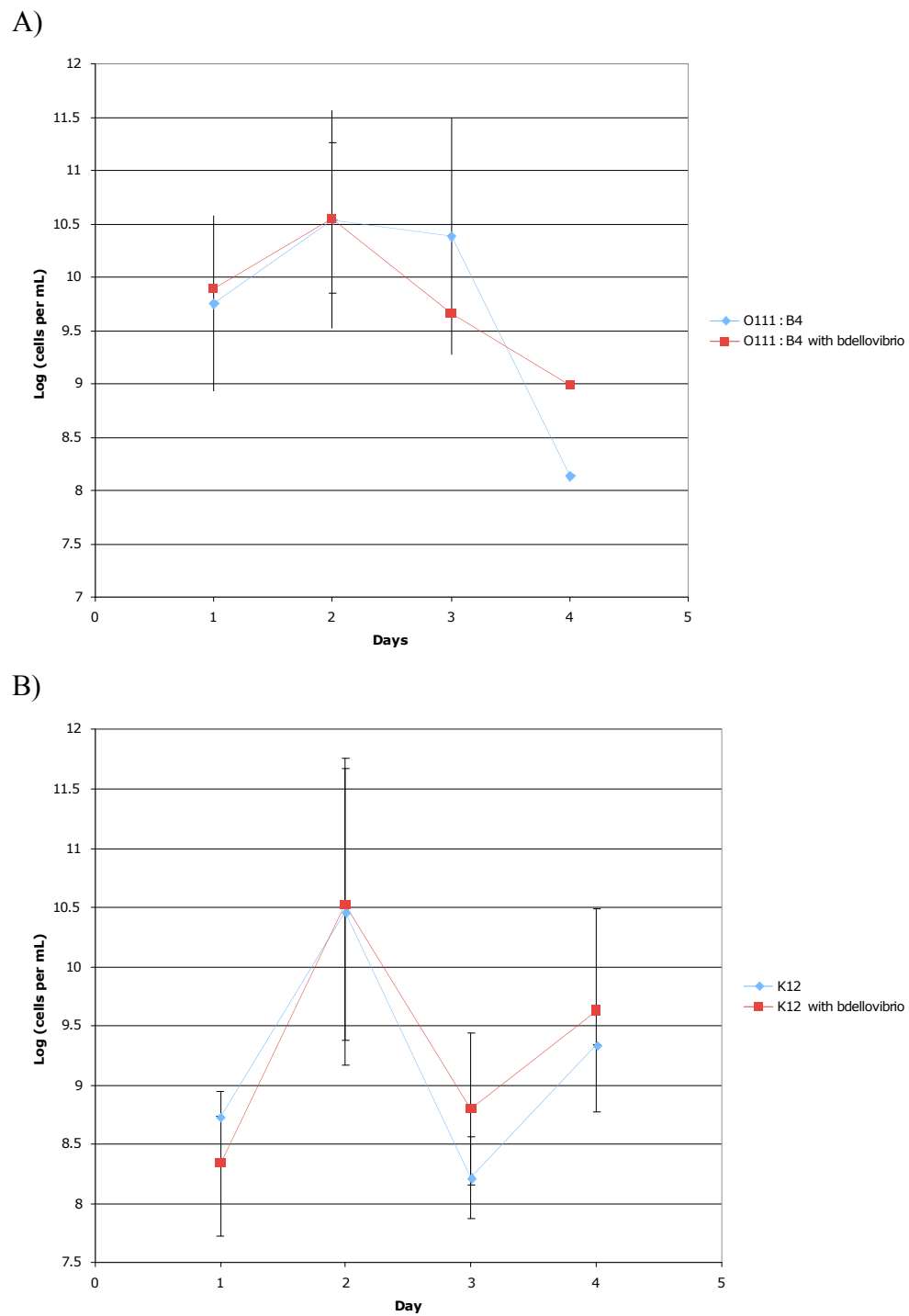


Figure 9: Cell counts for cultures grown with and without bdellovibrio. A) A graph showing the calculated number of cells per mL over a four day growth

cycle. This graph shows the amount of K12 present over a four day bdellovibrio growth cycle. Each point corresponds to a calculated amount of K12 in each suspension at a given time. Data are shown for suspensions with bdellovibrio present and suspensions without bdellovibrio present. B) A graph showing the calculated number cells per mL in two suspensions of O111:B4. This graph shows the numerous data for the suspensions of O111:B4 grown with and without bdellovibrio. Each data point is one calculated value for the number of O111:B4 cells present in the suspension.

points had a great deal of overlap. The inability to distinguish between data from the culture with bdellovibrio and the culture without means that no conclusions can yet be drawn about the predation of K12 by bdellovibrio. Though it is not reflected in the data, with light microscopy bdellovibrio were seen hunting in both the O111:B4 and K12 cultures.

## **Section 2: Developing a method for LPS preparation**

In order to successfully extract LPS from the rest of the cellular components, a method for monitoring the extraction process was needed. Several different methods were considered, but a set of three gels stained to monitor the amount of protein, DNA, and LPS was chosen to examine the multi-step extraction process. After each step (the extractions, dialysis, and centrifugations) a small sample was taken for use in the gels. For each extraction a 1% agarose gel was run to determine if DNA was present. Two polyacrylamide gels were run. One gel was stained with Coomassie Blue Stain to detect protein and the other was stained with silver salts to detect LPS. These gels allowed us to determine which molecule was present at each step during the extraction and determine what type of purification was necessary after the extraction was complete.

Originally, a Sepharose column was used to purify the final extraction product. The first effort with the silver staining procedure used to detect LPS was with the column fractions in which we attempted to determine the fraction

where the LPS came off the column. The fractions were combined into groups of ten and then run in two polyacrylamide gels. Each gel was stained with silver salts and photographed. As seen in Figure 10, the background was stained very dark and the bands only showed up when viewed on a light box. While it seems as though bands do appear in some of the fractions indicating that LPS is present, the LPS standard does not appear and, most importantly, the results could not be duplicated. However further examination of the gels from the extraction process indicated that there was minimal contamination of the original LPS solution and the column was not necessary.

The extraction process was analyzed by gel electrophoresis to reveal which molecules were present in each step. The first extraction was performed with the *E. coli* strain ML35. The process consisted of three extractions, a two-day dialysis, and three centrifugations. For the ML35 extraction, the agarose DNA gel showed very bright streaks of DNA in the first four lanes containing those samples that came from the extraction and dialysis steps (Fig. 11a). The next lane, which contains the supernatant of the first centrifugation step, contains almost the entire amount of the DNA present from the extraction. Some DNA is left over in the pellet, as is shown in the well of the pellet sample from the centrifugations but the remaining pieces of DNA are very large pieces of DNA that came out of solution and were collected with the LPS and stuck in the wells. The DNA band present in the pellet collected from the third centrifugation is brighter because the DNA

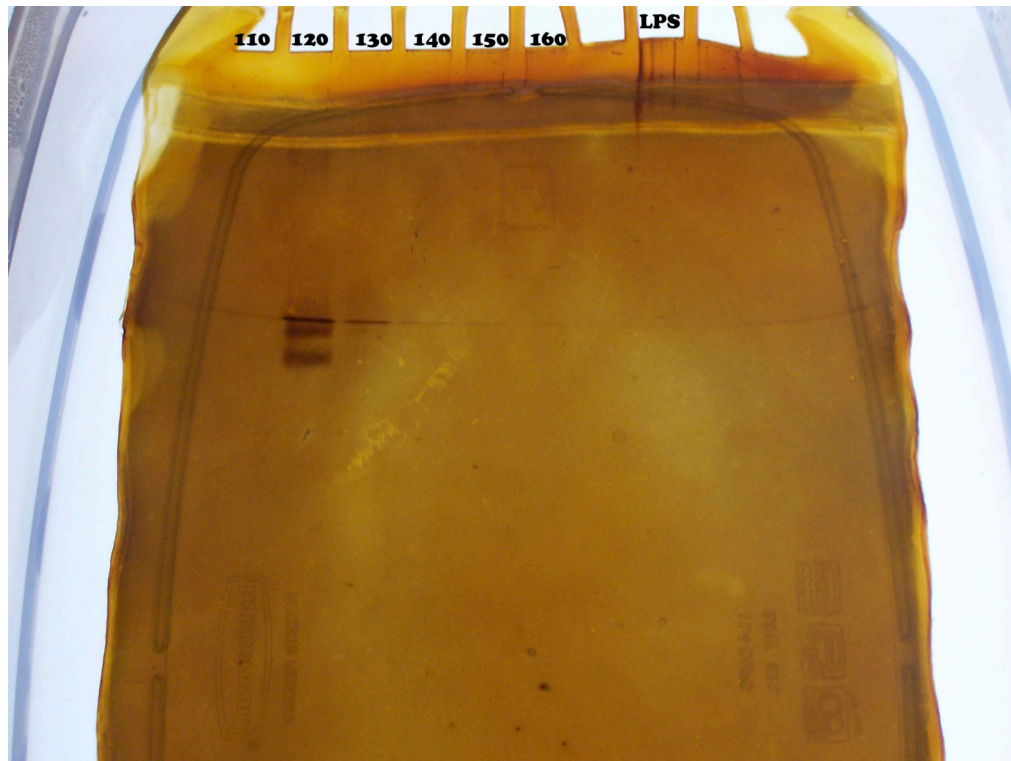
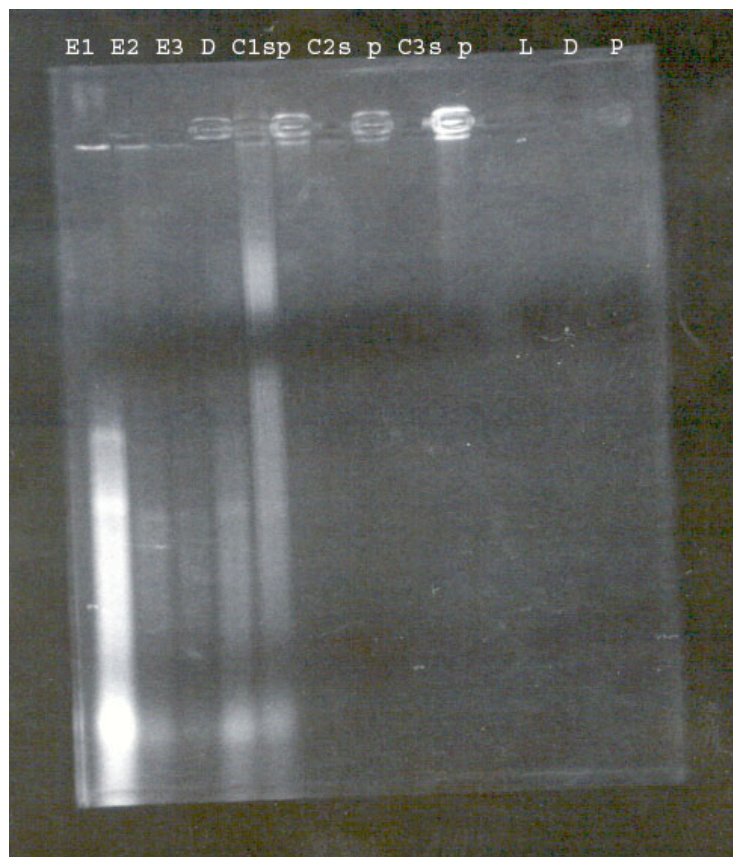
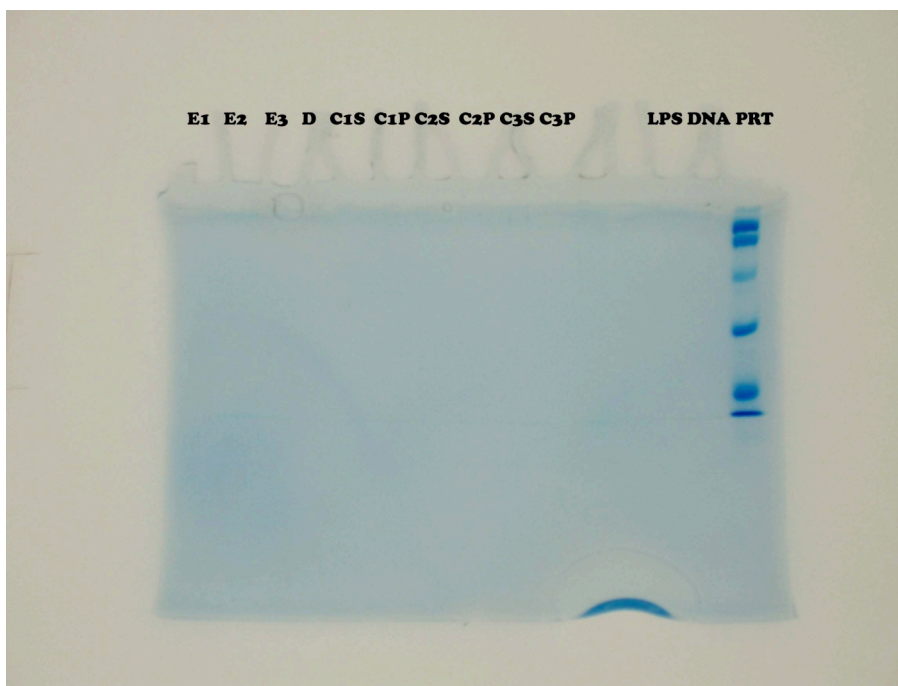


Figure 10: A polyacrylamide gel stained to detect LPS from the fractions of a Sepharose column. This gel is a polyacrylamide gel stained with silver to detect LPS. This gel contains fractions obtained from the Sepharose column, which have been labeled in groups of ten from 110 through 160. Fractions 120-140 seem to contain some LPS but the standard did not show up except as streaks at the top of the gel in the third lane from the right, labeled LPS. This has been seen in other gels as well; sometimes the LPS molecules get stuck in the stacking gel.

A)



B)



C)

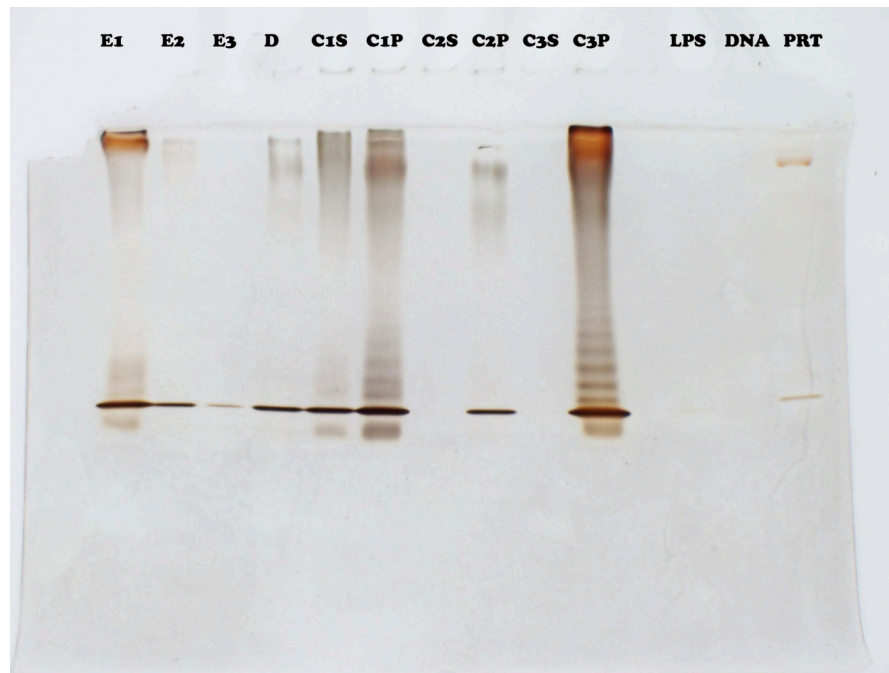


Figure 11: Protein, DNA, and LPS for the ML35 extraction process. These three electrophoretic gels were used to monitor the purity of each step in the extraction process of the ML35. Each sample has been labeled in each gel as follows: E1 is from the first extraction, E2 is from the second extraction, E3 is from the third extraction, D is from the dialysis step, C1S, C2S, and C3S are the supernatants of the first, second, and third centrifugations respectively, and C1P, C2P, and C3P are the pellets of the first, second, and third centrifugations respectively. These gels show that the final product is made up of LPS and a minimal amount of DNA. They also allowed the determination that the third extraction and centrifugation were unnecessary.

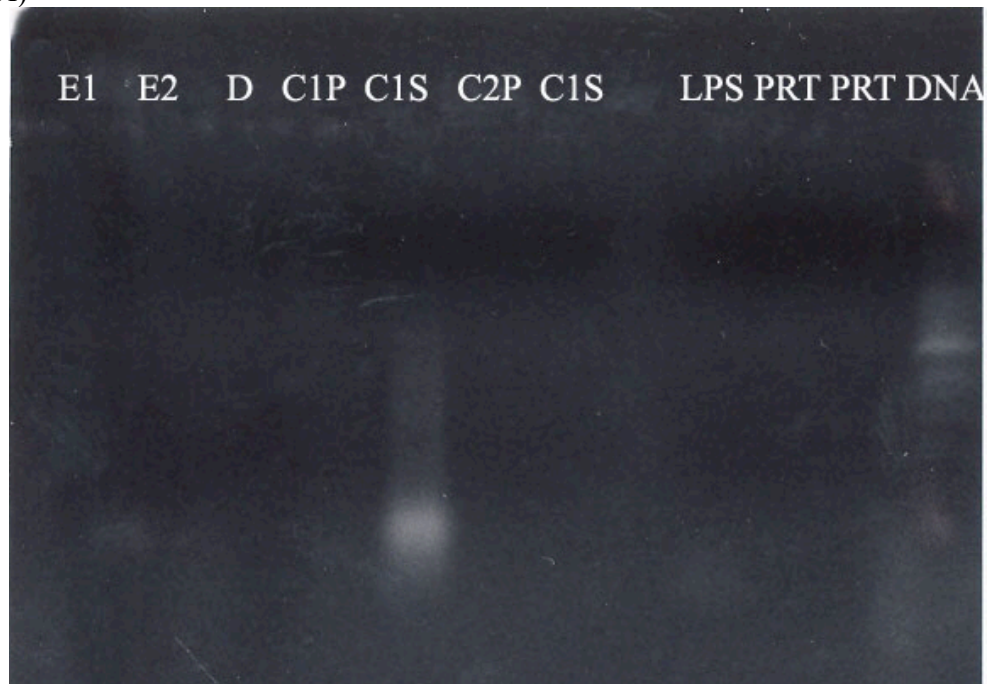
A) A is a 1% agarose gel in which DNA was imaged using ethidium bromide and UV light. The concentration of DNA present in each step (the extraction,

dialysis, and centrifugation) decreases until the final solution has a small amount of DNA present. B) B is a denaturing SDS 14% polyacrylamide gel that has been stained with Coomassie blue stain to detect any protein present in the extraction. The only lane that shows any protein is the low molecular weight protein standard. C) C is an identical denaturing SDS 14% polyacrylamide gel but this has been stained with silver salts to detect LPS. LPS was present in all of the extraction samples, the dialysis sample, and most of the centrifugation steps. The only two lanes of the extraction process that does not have LPS in them are the supernatants of the second and third centrifugation step. All of the supernatants were eventually discarded. Two bands of the protein standard appeared but the LPS standard did not.

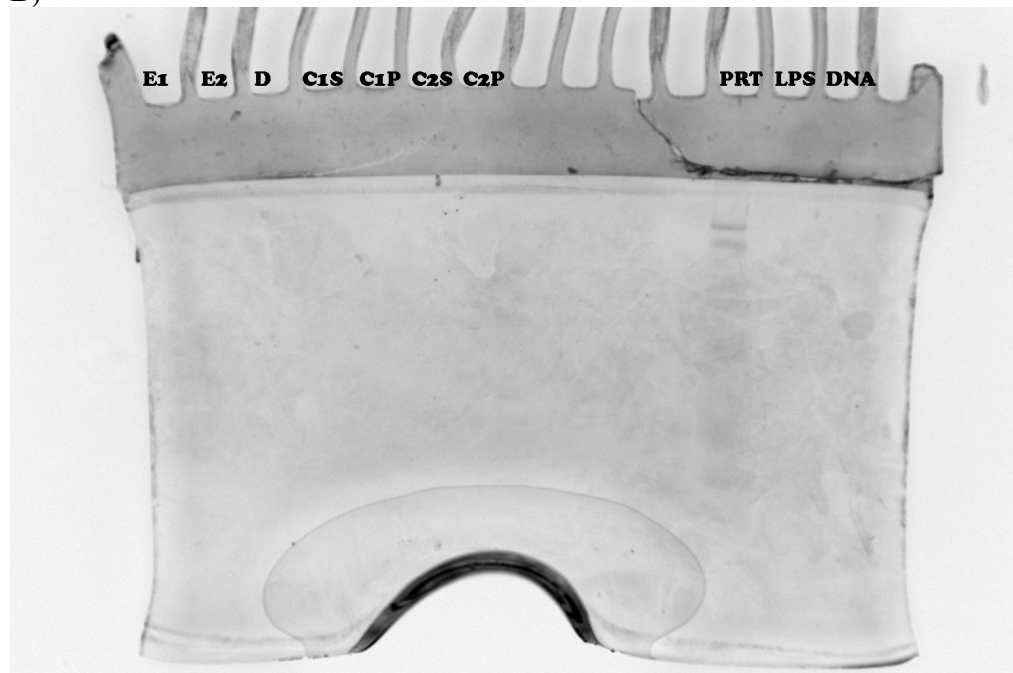
is present in a higher concentration though smaller amount than the other two centrifugation steps. None of the standards showed up, including the DNA ladder, which may have run off the bottom. The protein gel from the ML35 extraction shows no band in any of the samples (Fig. 11b). The background is slightly blue but the low molecular weight standard showed up very clearly. This means that there is no measurable amount of protein in any of the samples from this extraction. The LPS gel clearly shows that there is LPS present in several of the extracted ML35 samples (Fig. 11c). The first three lanes show that each extraction step collects diminishing amounts of LPS. The amount of LPS in the dialysect sample is quite high as it is a combination of all three extraction steps. Some LPS is obviously lost in the supernatant of the first centrifugation step, but most of it is contained in the pellet. The other two centrifugation steps are similar to the first. By the end of the entire process, a good sample of LPS was contained in the pellet of the third centrifugation. The LPS standard again did not show up but two bands of the protein standard did. The lack of selectivity of this staining procedure has been confirmed by other gels.

Similar sets of three gels stained to detect DNA, protein, and LPS were also run for the extractions of other prey LPS. The *bdellovibrio* (Fig. 12) and ZK1056 (Fig. 13) were extracted next and their gels were run and stained in tandem. Based on the results from the ML35 extraction the third extraction and the third centrifugation steps were eliminated. Both extraction

A)



B)



C)

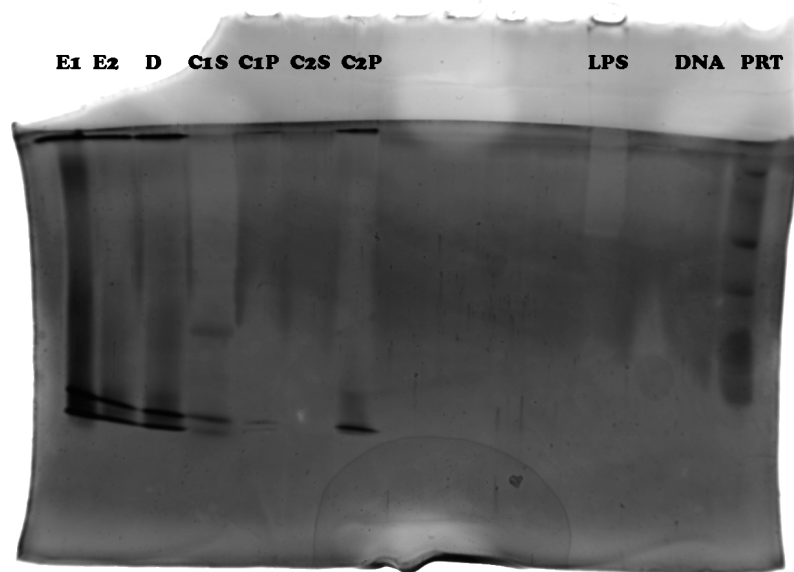
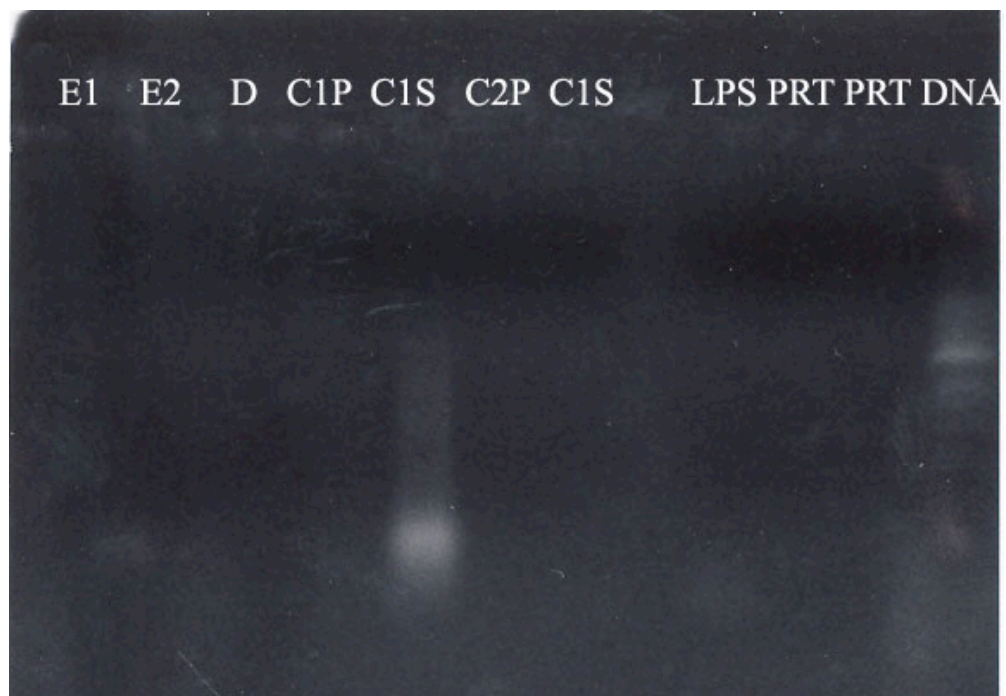


Figure 12: Protein, DNA, and LPS gels from the bdellovibrio extraction.

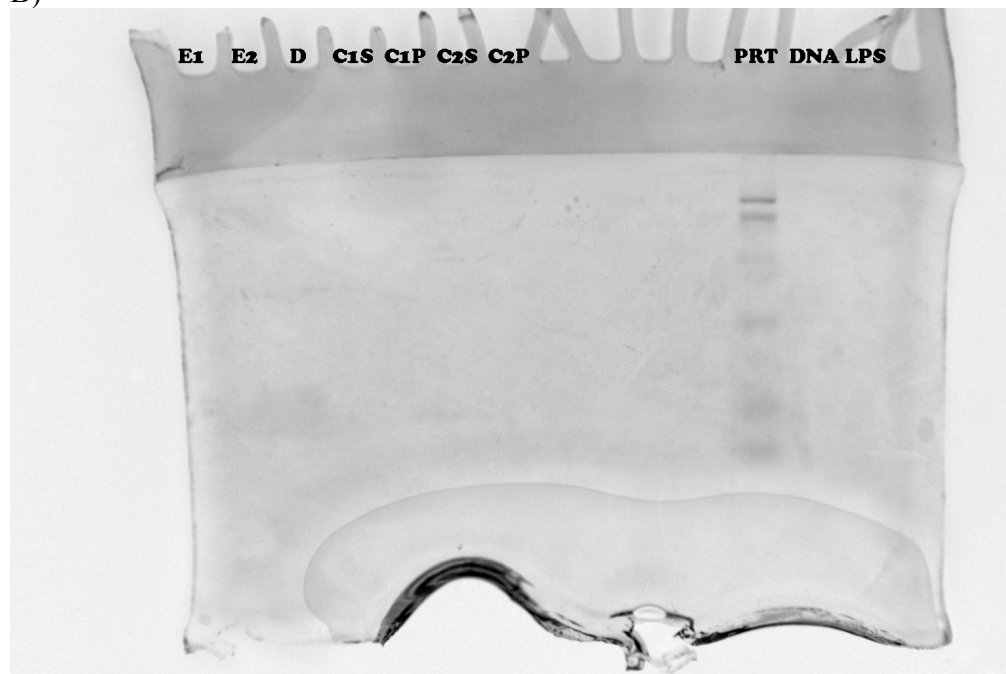
These three gels show the progression of the extraction of the bdellovibrio LPS. Each sample has been labeled in each gel as follows: E1 is from the first extraction, E2 is from the second extraction, D is from the dialysis step, C1S and C2S are the supernatants of the first and second centrifugations respectively, and C1P and C2P are the pellets of the first and second centrifugations respectively, similar to those in Figure 11. All three of these gels combined show that there is only LPS left in the final product. A) As seen in Figure 11, this 1% agarose gel has been imaged with UV light to visualize any DNA present in each extraction sample. Some DNA is removed in each extraction step but the majority of the DNA seems to be removed in the first centrifugation as the supernatant of the first centrifugation has the

highest amount of DNA. B) Again as seen in Figure 11, this denaturing SDS 14% polyacrylamide gel stained with Coomassie Blue Stain to detect any protein present in any of the samples. The only protein that appears is the low molecular weight protein standard. C) This denaturing SDS 14% polyacrylamide gel has been stained with silver salt to detect LPS. This gel has been over stained and in some instances is hard to detect, but there is LPS in the last extraction pellet.

A)



B)



C)

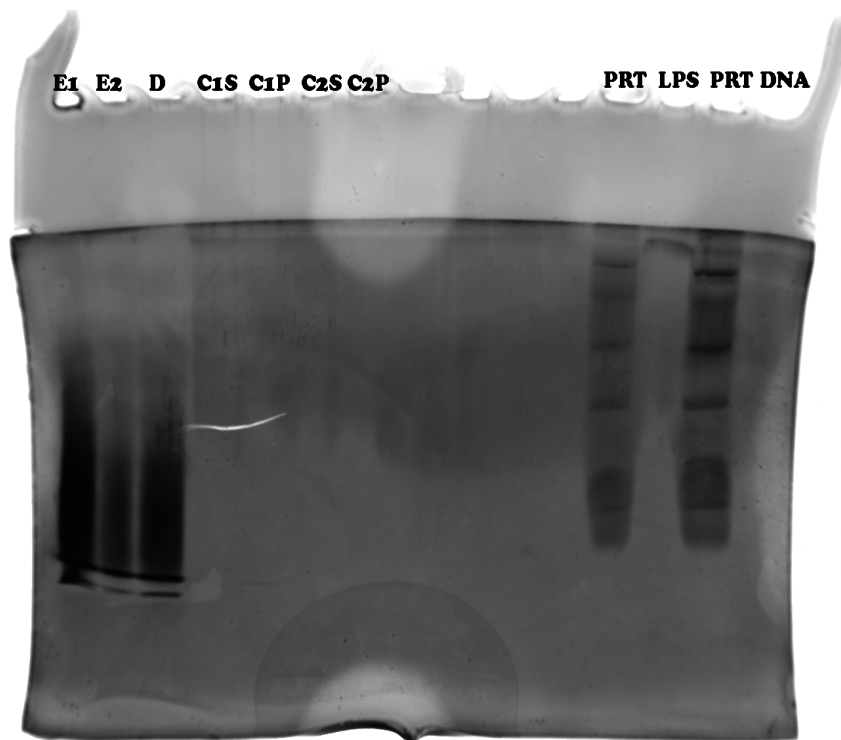


Figure 13: Protein, DNA, and LPS in the ZK1056 extraction process. These three gels monitor the extraction process of the ZK1056 bacteria. From these gels, it was determined that the final product is made entirely of LPS. Please refer to the figure legends of Figures 11 and 12 for specific information. A) This gel shows that most of the DNA was removed during the extraction and dialysis as those are the lanes that show the most DNA present. There is no DNA detectable in the final product. B) This gel shows that the only protein that is detectable is the low molecular weight protein standard. C) This gel is overexposed and it is hard to tell what is in each lane. There is a large amount of LPS in the first three samples but there is a small amount that can be detected

in the first pellet. The second pellet must have some LPS, but none shows up in the lane.

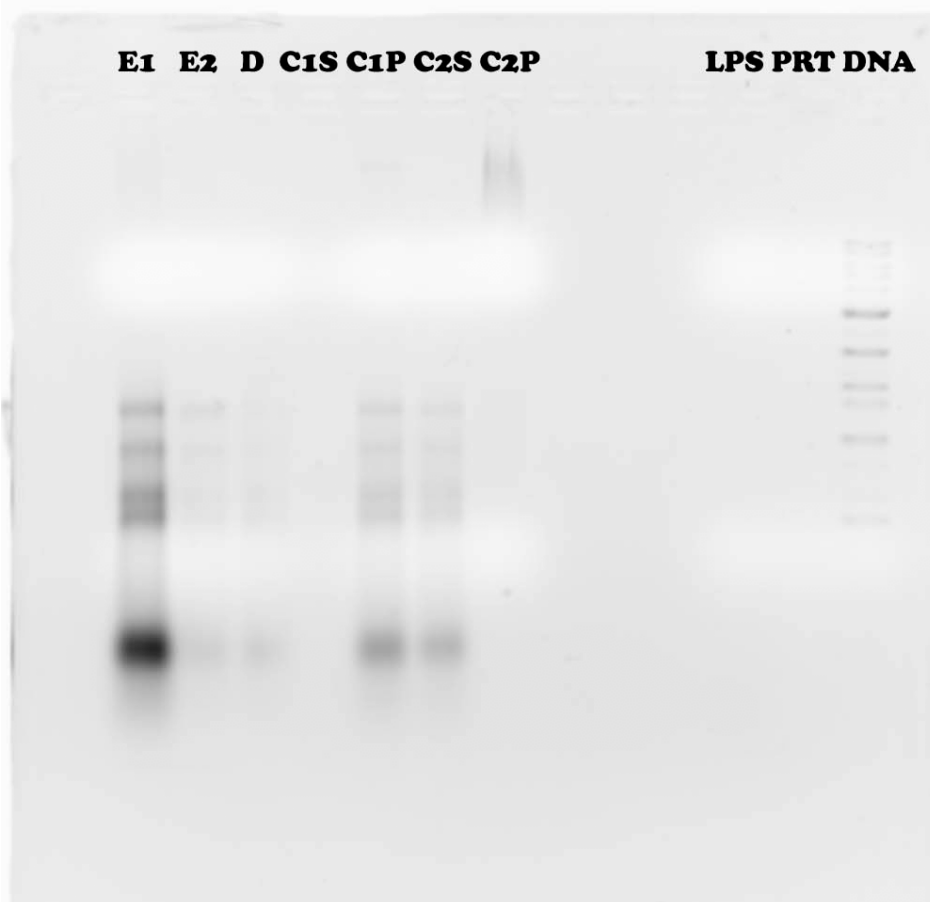
processes yielded results similar to those from the ML35 extraction. The ZK1056 and bdellovibrio extractions had no detectable DNA present in the final solution. As seen in Figure 12a, all of the visible DNA is removed from the bdellovibrio extraction process during the first centrifugation step. The DNA is not visible in either the extraction steps or the dialysis steps because the concentration was too low to be detected. Figure 12b shows a polyacrylamide gel stained to detect protein. The only measurable sample of protein was the low molecular weight standard. The polyacrylamide gel stained to detect LPS is shown in Figure 12c. In this gel, the LPS shows up clearly in the extraction samples and the dialysis sample. The LPS does not show up as clearly in any of the centrifugation samples. The absence of LPS staining is due to the low concentration of LPS in each sample. There is LPS in the final sample; it is faintly visible in the gel and there was a crystalline product after the final pellet was lyophilized.

In Figure 13a, an agarose DNA gel from the ZK1056 extraction process, DNA bands appear clearly in the extraction samples and the dialysis sample. No DNA appears in any of the other samples. This lack of detectable DNA appearing in the gel indicates that the DNA is present in a low concentration if it is present at all. Figure 13b shows a polyacrylamide gel stained to detect protein. The only protein that stains is the low molecular weight standard. This indicates that there is no measurable amount of protein in any of the extraction samples. The polyacrylamide gel stained to detect

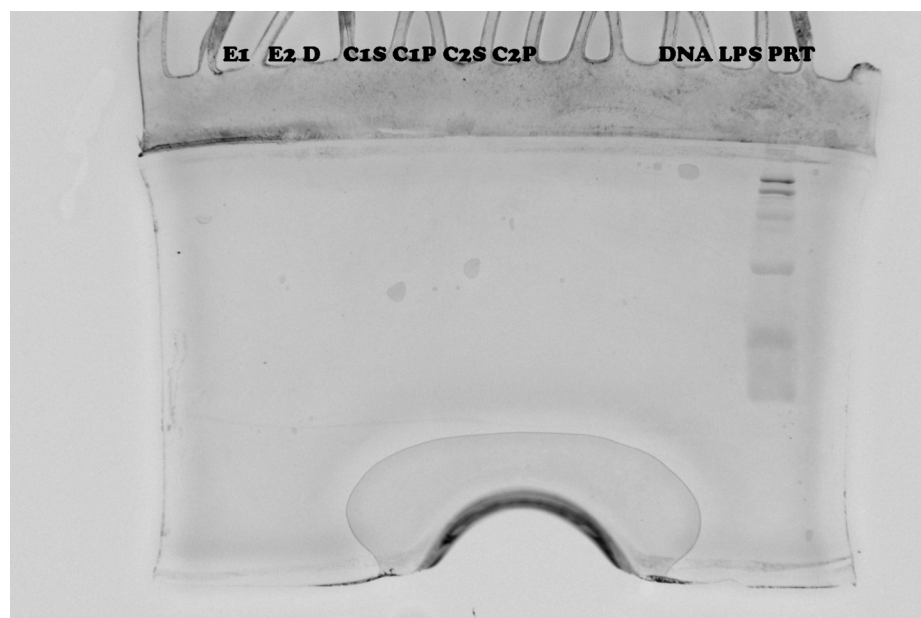
LPS is shown in Figure 13c. LPS appears in both extraction samples, the dialysis sample, the supernatant and pellet of the first centrifugation and the pellet of the second centrifugation. Two bands appear at the bottom of each lane. These bands may be due to LPS sticking in the well for a short time and then running on a slightly different time scale. The background of the gel is also stained.

The O111:B4 and K12 LPS were extracted and the gels were run and stained in tandem. Figure 14a shows the agarose DNA gel that contains samples from the K12 extraction process. DNA is present in the greatest concentration in the first extraction sample. It also appears to a lesser extent in the second extraction sample and the dialysis sample. The DNA remains in the pellet during the first centrifugation but most is discarded in the supernatant of the second centrifugation. A small sample of very high molecular weight DNA is present in the final sample. In Figure 14b, a polyacrylamide gel stained to detect protein, shows no detectable protein other than the low molecular weight protein standard. Figure 14c shows a polyacrylamide gel stained with silver to detect LPS. LPS is present in each sample except the supernatant of the first centrifugation. The dialysis sample has the highest concentration of LPS but some of the sample remained in the stacking gel. The protein standard appears faintly in the gel and the LPS standard appears in the last lane.

A)



B)



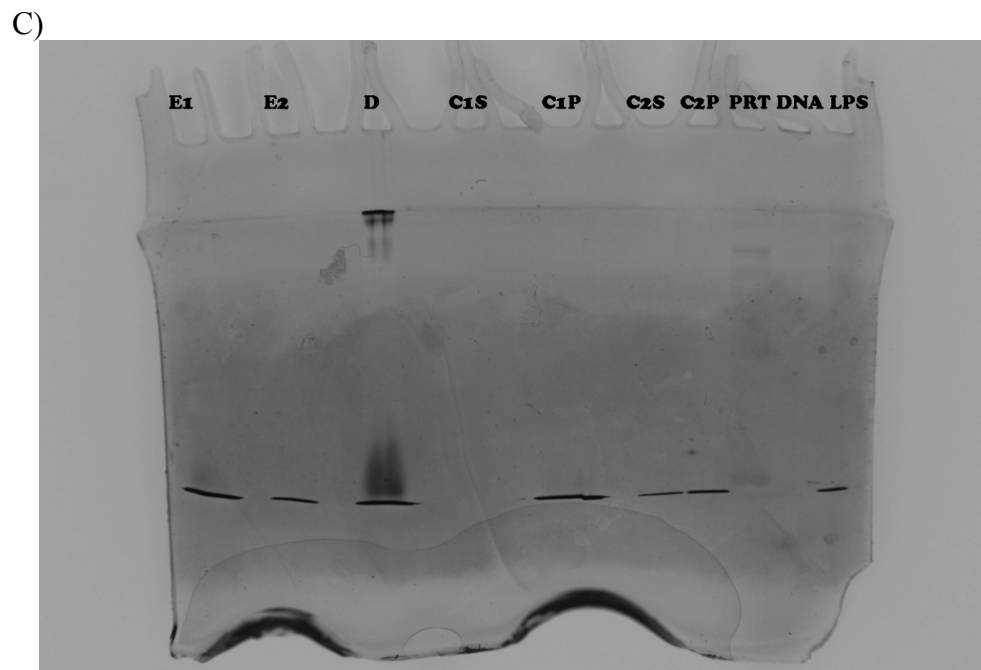
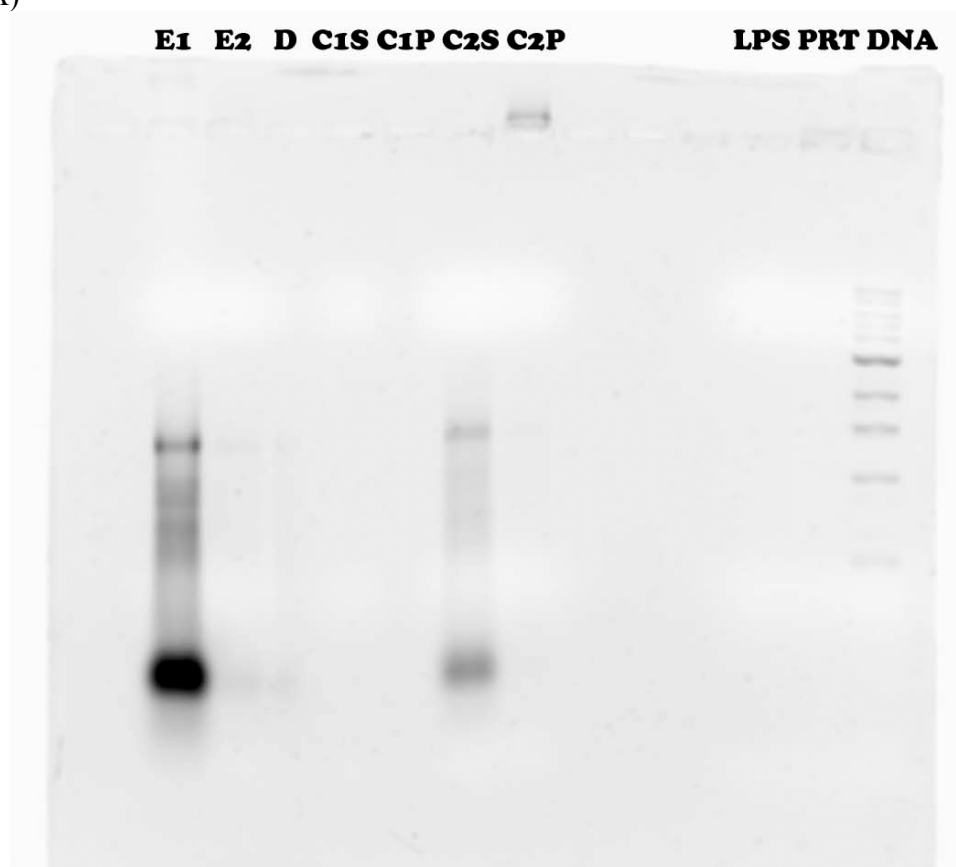


Figure 14: Protein, DNA, and LPS gels for the K12 extraction. These three gels were used to monitor the purity of the K12 extraction process. Please refer to Figures 11 and 12 for specific lane designations. When taken together, all three gels show that there is only LPS, with a negligible amount of DNA, in the final product. A) This gel 1% agarose gel shows any DNA that has been left after the second centrifugation are very large pieces that came out of solution. B) This polyacrylamide gel shows there is no protein present in any of the extracted samples. The only protein that appears is the low molecular weight protein standard. C) This a polyacrylamide gel which shows there is LPS in every sample except for the supernatant of the first centrifugation. Some LPS is obviously lost as a band is visible in the supernatant of the second centrifugation in lane 11. The protein standard also appears.

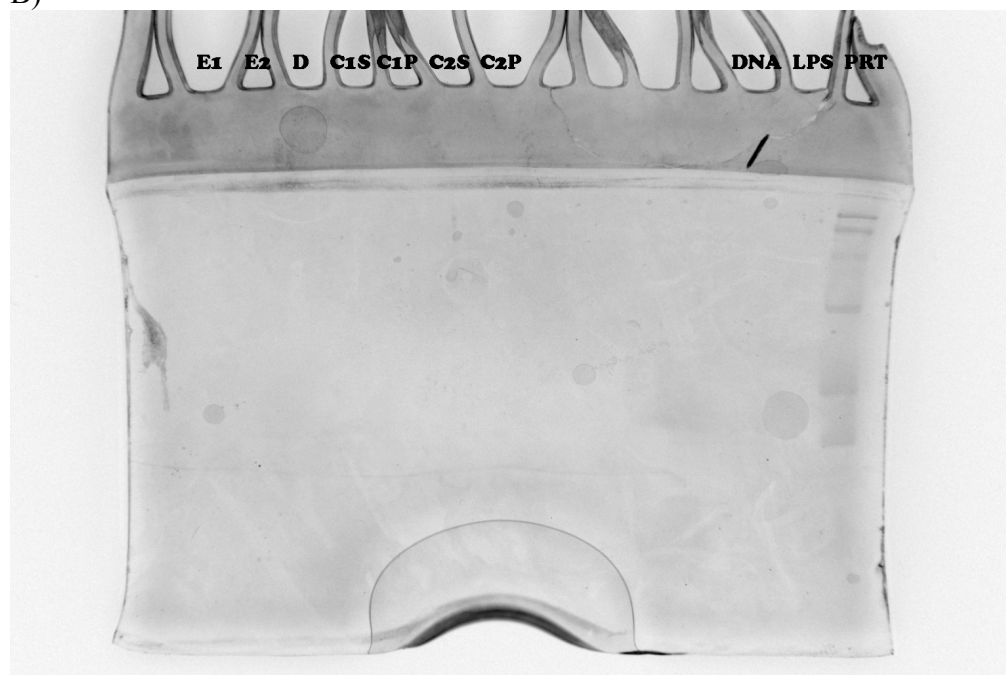
Figure 15 shows the gels used to monitor the O111:B4 extraction process. In Figure 15a, a high concentration of DNA is present in the first extraction sample. There is also a lower concentration of DNA in the second extraction sample and the dialysis sample. DNA bands are present in the supernatant of the second centrifugation, but not in either of the first centrifugation samples. Some DNA is present in the final pellet, as is shown in the well of sample from the pellet of the second centrifugation. The polyacrylamide gel stained with Coomassie blue stain shown in Figure 15b shows no detectable protein except for the protein standard in the last lane. Figure 15c, a polyacrylamide gel stained with silver to detect LPS, shows a high concentration of LPS in both the first and second extraction samples. There is a much lower concentration of LPS in the dialysis sample. Some of the detected LPS of the dialysis sample is stuck in the well. There is no detectable LPS in the supernatant of the first or second centrifugation and only a small amount of detectable LPS in the pellet of that centrifugation. The concentrations of these samples were most likely too low to be detected. There is a higher concentration in the pellet of the second centrifugation sample. The protein standard appears faintly as does the LPS standard.

In summary, though different in strain and isolations, the final LPS from each strain was relatively pure. There was no detectable protein present in any sample and only three of the samples had any DNA present (Fig. 11-15).

A)



B)



C)

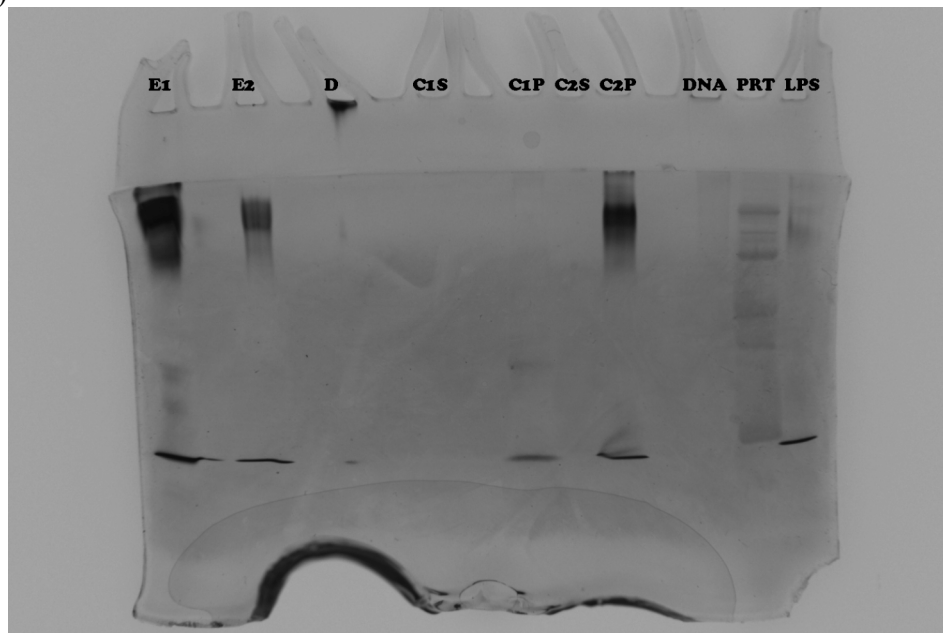


Figure 15: Protein, DNA, and LPS in the O111:B4 extraction. These three gels were used to monitor the extraction process of the O111:B4 LPS. Please refer to the figure legends of Figures 11 and 12 for specifics. These three gels show that the final extraction product is made up almost entirely of LPS with a very small amount of DNA. A) This gel shows that any DNA that has been left after the second centrifugation are very large pieces, so large they couldn't migrate out of the well. B) This polyacrylamide gel shows there is no protein present in any of the extracted samples. The only protein that appears is the low molecular weight protein standard. C) This polyacrylamide gel shows there is LPS in every sample except for the supernatant of the first and second centrifugation. The LPS from the dialysis sample seems to have gotten stuck in the stacking gel and the protein standard also appears.

### Section 3: Comparison of Bacterial LPS Types

Polyacrylamide gel electrophoresis with silver staining was used to examine the differences between the eight different LPS types. LPS from six of the seven prey organisms were run side-by-side on the same gel (Fig. 16). This gel, though incomplete, does give some valuable information. The distinction between rough strain LPS and smooth strain LPS is clearly visible on this gel. The ZK1056 and the EH100, a known rough strain, are clearly missing the upper bands that the O111:B4, a known smooth strain, the ML35, the bdellovibrio, and the *Pseudomonas aeruginosa*, another known smooth strain. The O111:B4 LPS and ML35 LPS show some bands in the lanes next to the main sample due to overflow while loading. The sample in these lanes has a lower concentration than the main lanes. The O111:B4 has at least 4 bands present in the lower half of the LPS sample while the ML35 has at least 5 bands present in the lower half of the LPS sample. The new *Pseudomonas aeruginosa* sample, ordered from Sigma six months after the old *Pseudomonas* sample, stains darker than the old sample. The lipid A did not appear at all.

### Section 4: Supported lipid monolayers

LPS molecules purchased from Sigma and extracted LPS molecules were used to form monolayers on alkylated glass cover slips. By placing the LPS monolayers on an air water interface and pushing the silanated cover slip

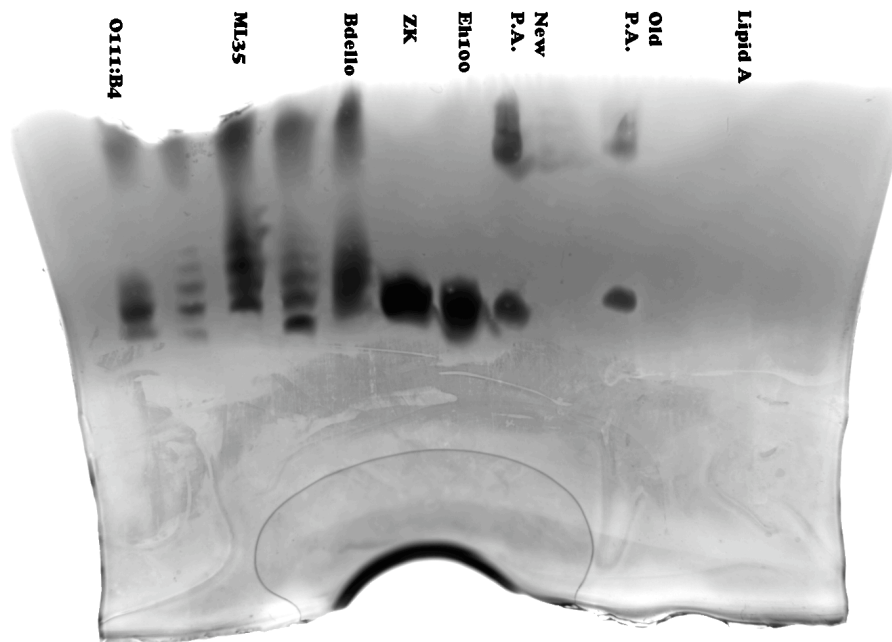


Figure 16: A polyacrylamide gel showing six different LPS. This image shows six of the eight LPS strains, all of which are labeled at the top of the wells. The O111:B4 seen here is that purchased from Sigma. Here, it is the remainder from the actual sample seen in the well to the right of the O111:B4 and the ML35, shows bands while the sample does not. The P.A. is the *Pseudomonas aeruginosa* LPS.

through that interface a single layer of LPS molecules is deposited on the glass with tails of the lipid A moiety contacting the alkylsilane. The excess LPS at the interface was removed using an aspirator leaving fluid to cover the cover slip. The monolayers were imaged using contact AFM under fluid.

Before the monolayers could be imaged, controls were established so that the monolayer would be recognized in comparison. First clean glass was imaged. The cleaned glass images were fairly uniform, though not entirely flat (Fig. 17). There were some rough areas and dust particles visible with a depth or “z scale” of 10 nm when viewed in air, but the dust particles disappeared under water. The next control imaged was alkylated glass (Fig. 18). The alkylated glass was also very uniform with a z scale of 10 nm, though it was hard to image because the alkyl groups tended to stick to the AFM tip causing the tip to lose contact in places. As time passed, a higher number of dust particles attached to the slide. It proved impossible to image the alkylated glass under fluid.

The first layers imaged with the AFM were the phosphatidyl choline (PC) layers. Although the PC is dissimilar to the LPS we want to study because it lacks sugars and has fewer fatty acid tails, these simple amphipathic phospholipids are inexpensive and are known to form stable monolayers. We were able to demonstrate monolayer deposition and AFM characterization. As seen in Figure 19, the PC monolayers were uniform and entirely uninteresting at a z scale of 10 nm imaged in fluid. The monolayers were flat,

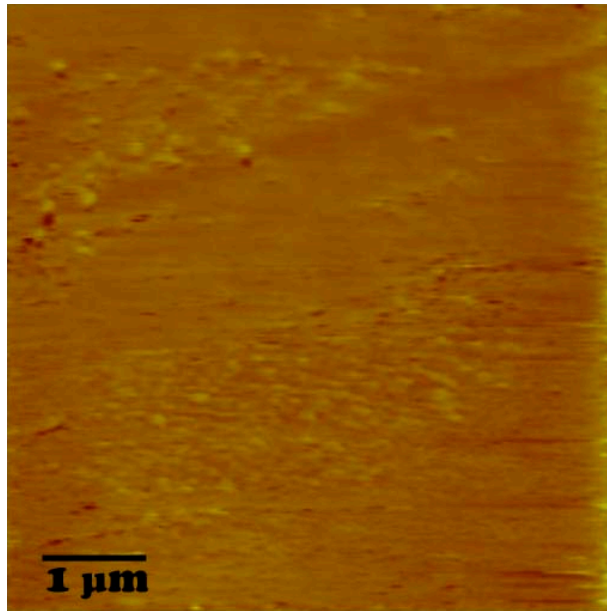


Figure 17: Clean glass imaged with contact AFM. This figure shows glass cleaned with sulfuric acid and Nochromix visualized with AFM. This height image measures 6  $\mu\text{m}$  high by 6  $\mu\text{m}$  wide. The glass was observed under water in the same way the LPS monolayers would be. This image has been flattened using the software provided with the AFM.

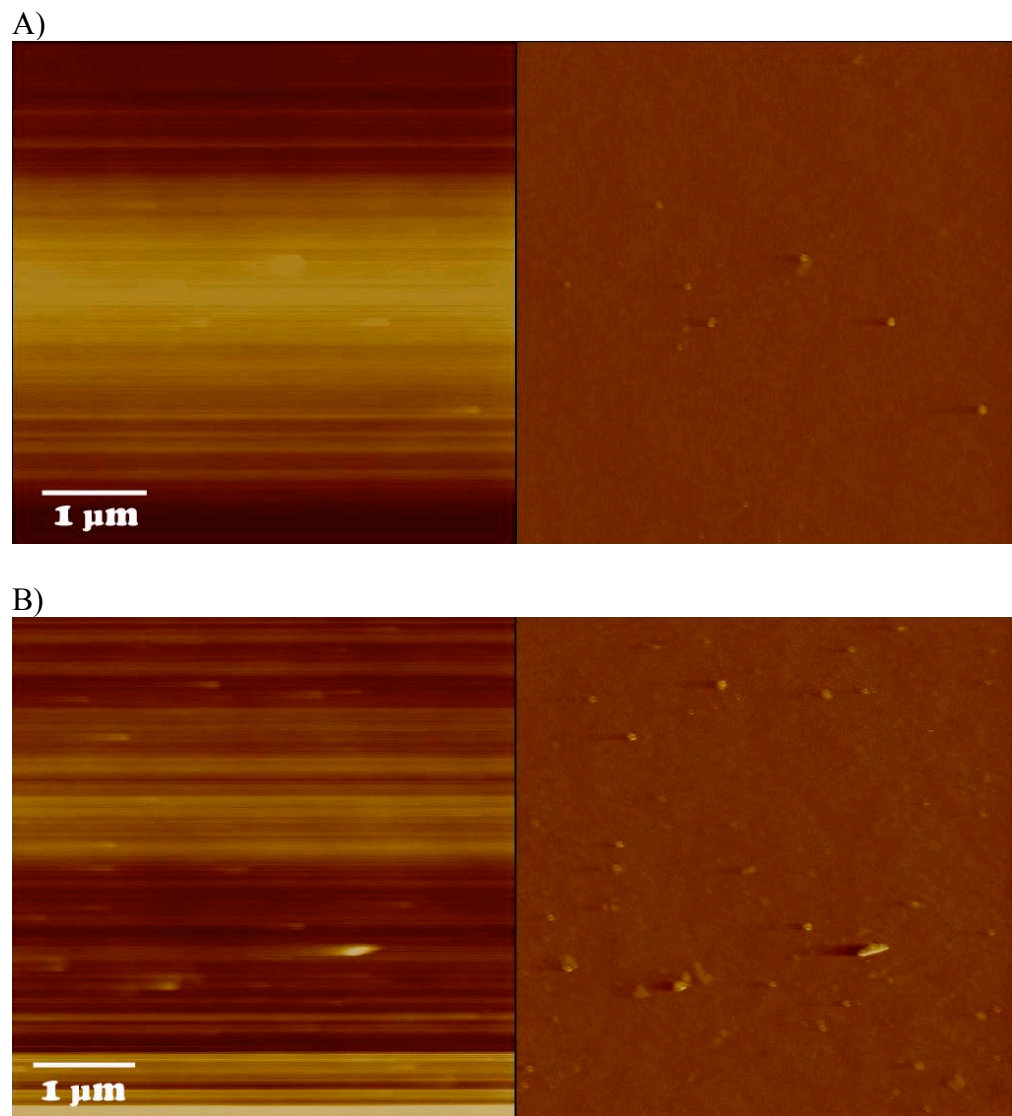


Figure 18: AFM images of alkylated glass. These images are of cleaned glass treated with an alkyl silane to make them hydrophobic. Their hydrophobicity does not allow for them to be imaged under fluid in a method consistent with the LPS monolayer. In both images A and B, the left image is the height image and the right image is a deflection image. Each section of both images (height and deflection) measure  $5\ \mu\text{m}$  tall by  $5\ \mu\text{m}$  wide. Both images have been flattened. Image A is an initial picture of the silanated surface and image

B is the same area after half an hour of sitting on the AFM. Dust particles have collected over that time.

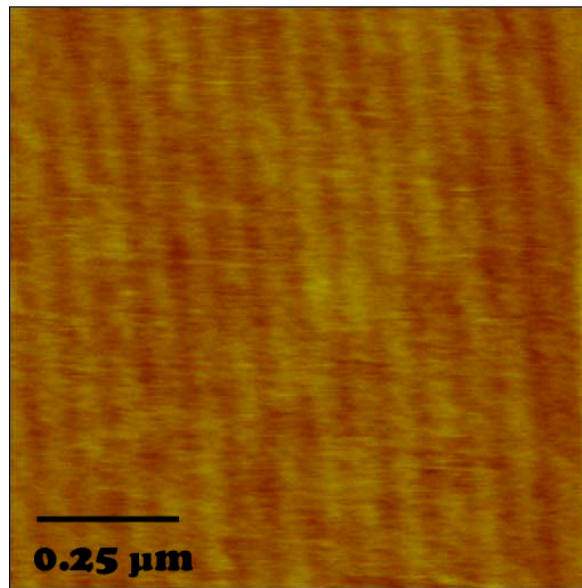


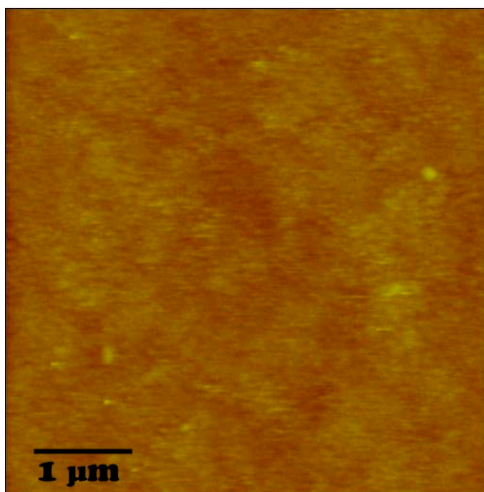
Figure 19: An image of a PC monolayer imaged with AFM under fluid. This image is of a PC monolayer imaged under water by contact mode AFM. The image is 1 micron by 1 micron in size and has been imaged at a height of 10 nm. The monolayer is actually flat, the appearance of crests in the image is created by instrument noise during the imaging process. This image has been flattened.

fluid, and had good coverage of the glass surface. When we tried to scratch a hole in the monolayer to measure its depth, the lipids would move back into the area that had previously been cleared within the scan time (about 10 minutes).

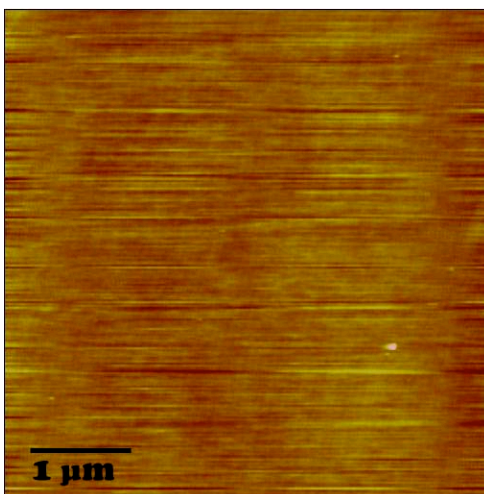
Next we prepared monolayers of LPS. The smooth LPS monolayers created with the head groups facing out formed consistent layers with good overall coverage (Fig. 20). There are no visible holes in these monolayers, which would appear as areas where the tip would lose contact with the monolayer. There is some difference in the heights within the individual images of the monolayers, which is to be expected as the O-antigens are not only heterogeneous in size but are moving in the water and may show up as different heights in the image. These images were also very fluid. When a section of the monolayer was scratched off to determine the depth of the monolayers, the molecules returned to the area too quickly and no image of a hole could be captured (Fig. 21).

Images from an isolated lipid A appear in Figure 22. The lipid A molecules were isolated from the extracted ML35 LPS by acid hydrolysis. They were deposited onto the alkylated glass in the same manner as the LPS molecules. It was similar in appearance to the LPS monolayers. It is flat at a z scale of 10 nm. As with the LPS monolayers, no holes were present in this monolayer.

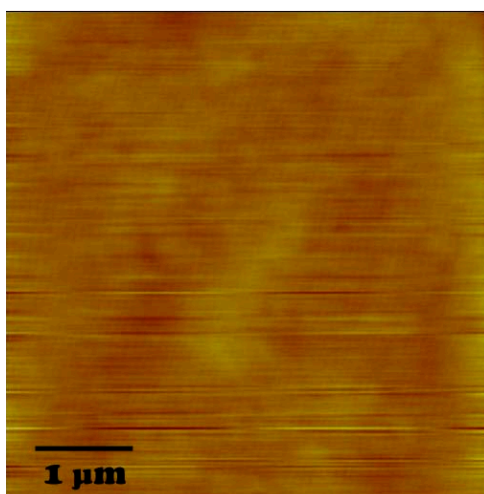
A)



B)



C)



D)

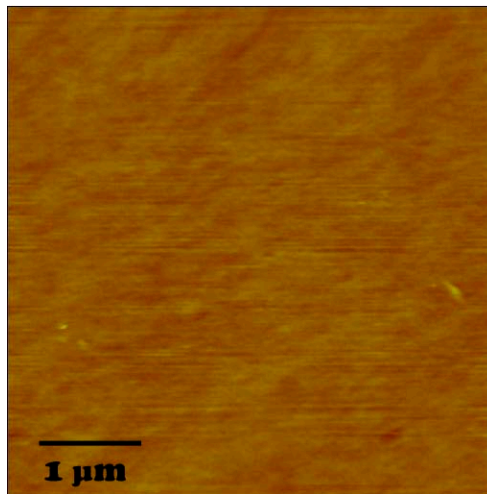


Figure 20: AFM images of monolayers formed with smooth strain LPS.

These images are of smooth LPS monolayers made with the O-antigens facing out. Each image has a z scale of 10 nm and measured 5 μm by 5 μm. These images have been flattened. A) O111:B4 LPS monolayer. B) ML35 LPS monolayer. C) *Bdellovibrio* LPS monolayer. D) *Pseudomonas aeruginosa* LPS monolayer.

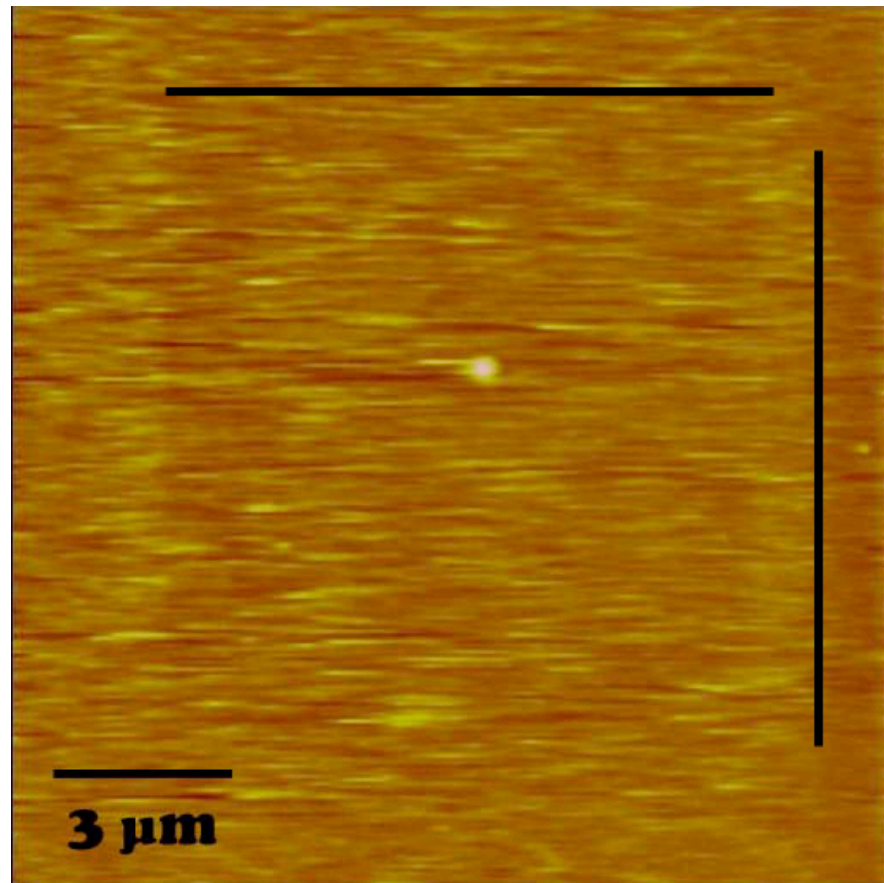


Figure 21: An image of a scratched LPS monolayer. This image is of a LPS monolayer made with FITC-labeled O111:B4 LPS with the O-antigens facing out and was imaged under fluid. The image is 15  $\mu\text{m}$  by 15  $\mu\text{m}$ . A scratched area of 10  $\mu\text{m}$  by 10  $\mu\text{m}$ , indicated by the lines, is faintly visible in the center of the image. However, the glass is still covered with a monolayer. The LPS molecules have simply been pushed toward the side of the scratched area and no hole has appeared in the monolayer. This image has been flattened.

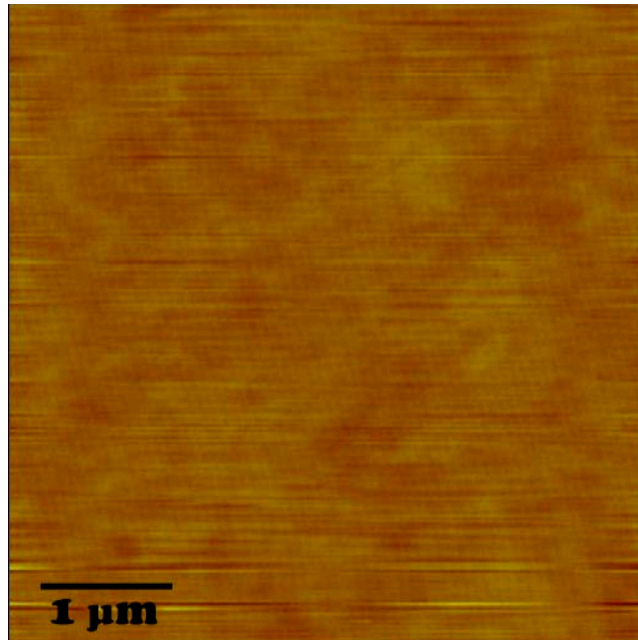


Figure 22: A monolayer formed with lipid A and imaged with AFM. This image is of a monolayer formed from lipid A isolated from ML35 LPS with the head of the lipid A facing out. The image measures 5  $\mu\text{m}$  by 5  $\mu\text{m}$  and has a z scale of 10 nm. This image has been flattened. There are some slight disturbances caused by either the tip or a liposome at the bottom of the image.

The rough strain LPS monolayers appeared very similar to the smooth LPS monolayers. The rough strain monolayers were formed and imaged in the same manner as the smooth strains. Figure 23 shows the available rough LPS monolayers imaged under fluid. Both images were flat at a z scale of 10 nm.

To further characterize the LPS molecules, monolayers were also formed with the fatty acid tails facing out. The LPS monolayers were formed by placing LPS molecules at the air water interface as before. To face the tails out, a piece of freshly cleaved mica was placed under the air water interface and pulled through so that the head groups touched the mica. These monolayers were then imaged in air using contact AFM.

As with the monolayers formed with the heads out, controls first needed characterization. Mica was imaged as seen in Figure 24. The mica is extremely flat; it is flat on a molecular level. The z scale of the image is 10 nm.

The tails out monolayers formed two distinct types of monolayers depending on whether the LPS was rough or smooth. The rough strains ZK1056, EH100, and K12, had domains appearing in the monolayer while the smooth strains, O111:B4, ML35, and *bdellovibrio*, usually formed a uniform monolayer. The spots in the rough strain monolayers varied in size depending on the strain as seen in Figure 25. Each of these monolayers has different size and shape to the domains. The domains in the EH100 were circular and had

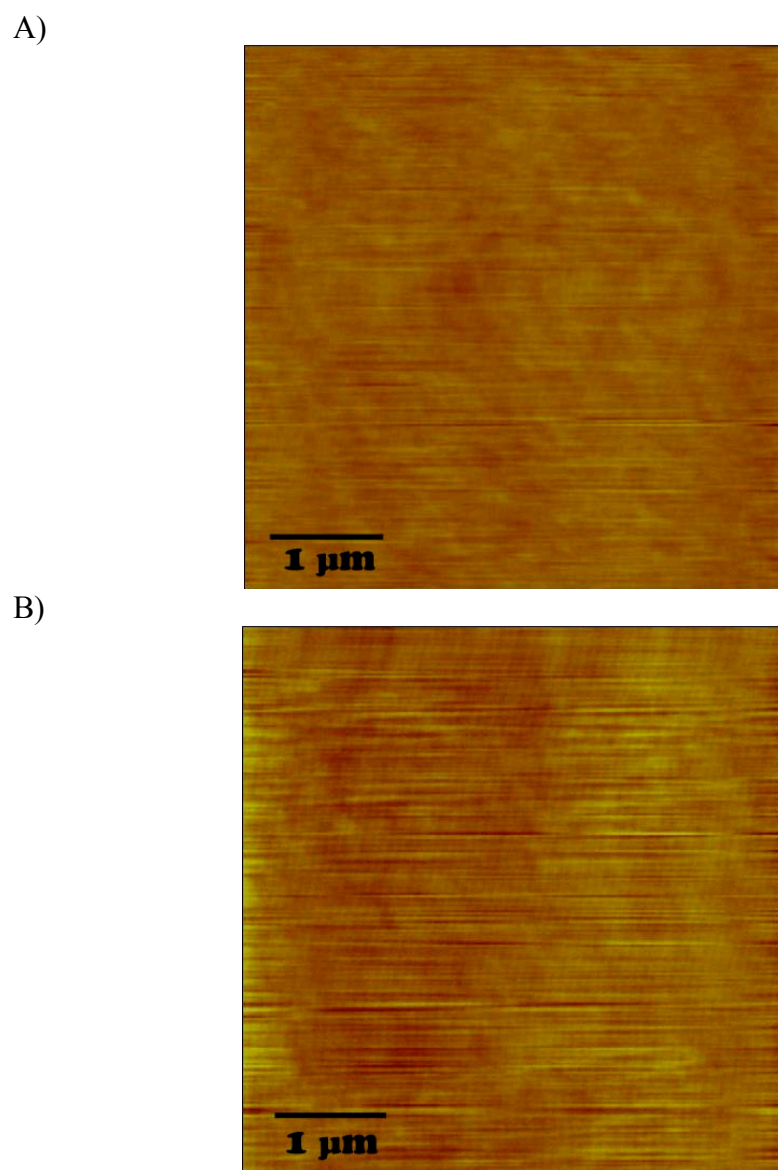


Figure 23: Images of rough type LPS monolayers prepared with the heads facing out. Each contact image is a height image with a z scale of 10 nm. The images are each 5  $\mu\text{m}$  by 5  $\mu\text{m}$ . These images have been flattened. A) EH100 LPS monolayer. B) ZK1056 LPS monolayer.

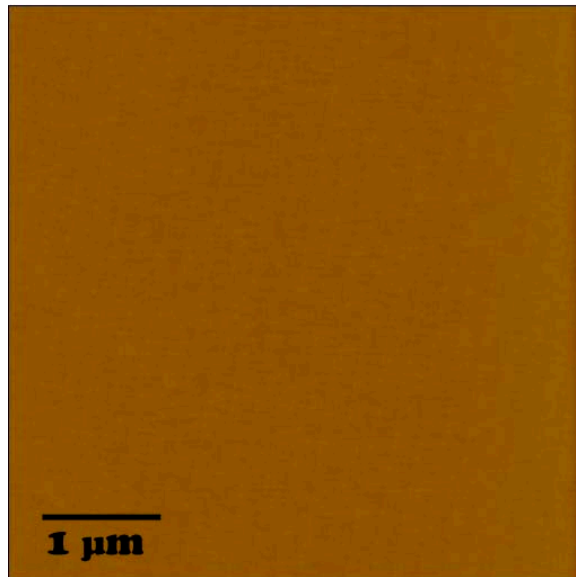
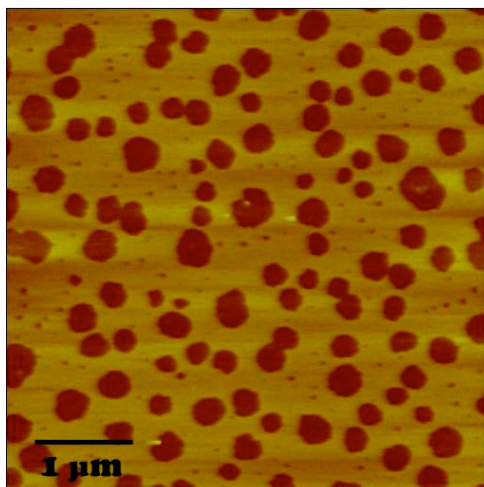
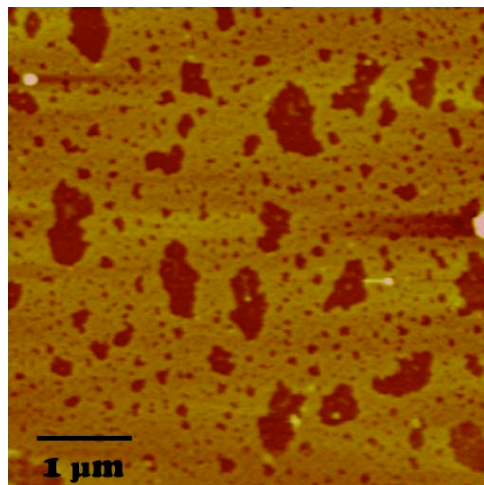


Figure 24: An image of freshly cleaved mica imaged in air by AFM. The image measures 5  $\mu\text{m}$  by 5  $\mu\text{m}$  and has a z scale of 10 nm. This image has been flattened. It is obvious that this substrate is much flatter than the other substrate, the cleaned glass. This makes sense as mica is a molecularly flat material while glass is not.

A)



B)



C)

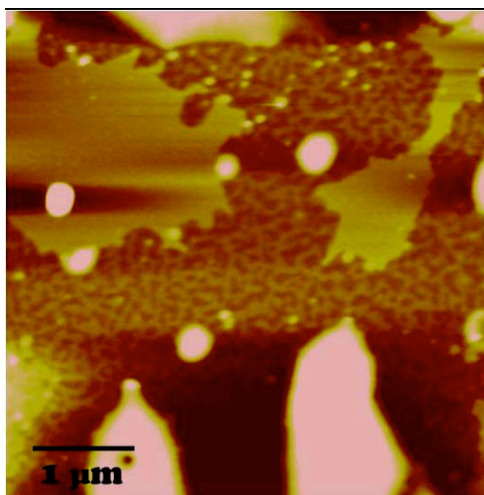


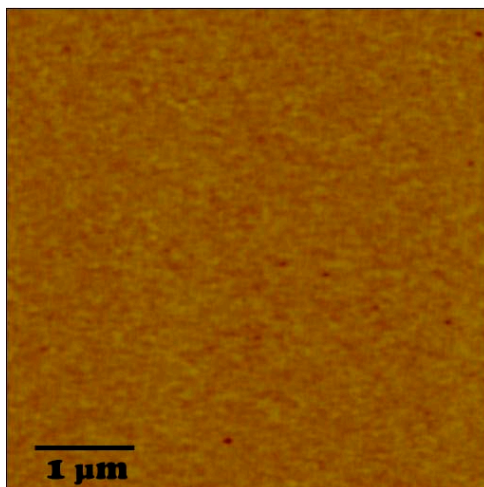
Figure 25: Images of rough strain LPS monolayers formed with the fatty acid tails facing out. Each image of these monolayers formed with rough LPS measures 5  $\mu\text{m}$  by 5  $\mu\text{m}$  and has been flattened. The z scale is 10 nm. A) EH100 LPS monolayer. B) ZK1056 LPS monolayer. C) K12 LPS monolayer. While there are large liposomes, the actual monolayer that has been formed in the background is the best illustration (so far) of the types of monolayers that this LPS strain is forming.

an average size of approximately 0.25  $\mu\text{m}$  in diameter though some were much smaller. The domains in the ZK1056 monolayer were 0.05  $\mu\text{m}$  to 0.5  $\mu\text{m}$  in diameter, though the domains were not as circular as those found in the EH100 monolayer. These domains were more oblong and did not have the smooth edges that the EH100 had. The K12 domains are roughly 0.1  $\mu\text{m}$  in diameter but the domains are obscured by large vesicles. However the domains appear clearly in the image behind the vesicles. The K12 domains do not appear to have a regular shape. Some of them are round, some are oblong, and others have a boomerang-like shape to them.

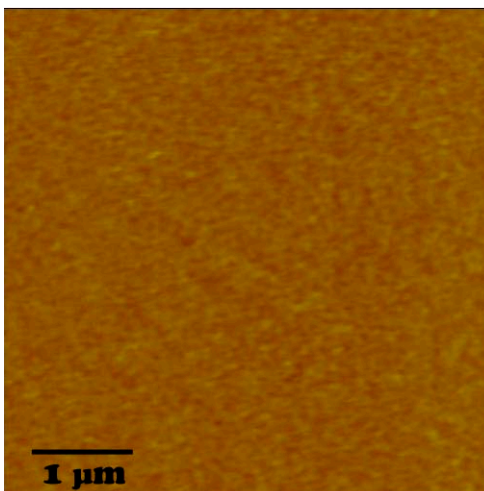
The monolayers made from smooth strains were all very similar in appearance. These monolayers were very smooth, yet still appeared slightly different than those monolayers imaged under fluid (Fig. 26). The O111:B4, ML35, and *bdellovibrio* monolayers have a slightly bumpy appearance with a z scale of 10 nm. The *Pseudomonas* has a bumpier appearance than the other three monolayers. These bumps are not caused by liposomes which would be removed after one image was taken. Importantly, these bumps appeared in the same area over multiple scans. These bumps could be caused by the variation in the number of repeating O-antigen units LPS molecules. This difference in size could cause a bumpy appearance.

Though different in appearance, both monolayers were fixed. These monolayers could have holes scratched in them *without* the molecules moving back into the scratched area. This was also apparent in that the monolayer

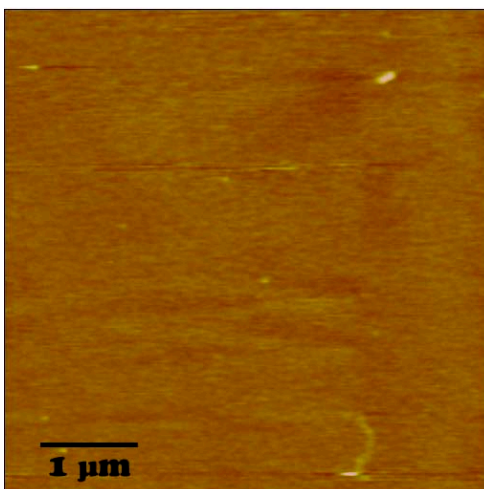
A)



B)



C)



D)

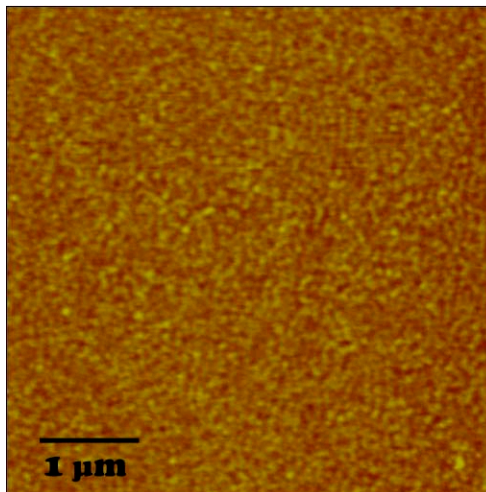


Figure 26: Images of smooth LPS monolayers formed with the tails out.

These images are of the smooth type LPS monolayers with the fatty acid tails out. Each image has a z scale of 10 nm and measures 5  $\mu\text{m}$  by 5  $\mu\text{m}$ . These images have been flattened. A) O111:B4 LPS monolayer. B) ML35 LPS monolayer. C) *Bdellovibrio* LPS monolayer. D) *Pseudomonas aeruginosa* LPS monolayer.

would not move if the same area was imaged more than once. When a monolayer with the heads out was imaged multiple times and a distinguishable feature such as a liposome was present, the liposome was observed moving across the monolayer as the images progressed. This was not observed in the “tails out” monolayers. Any distinguishable feature in the tails out monolayers did not move across the monolayer as the images progressed.

Lipid A was also used to form a monolayer with the fatty acid tails facing out (Fig. 27). This lipid A sample was purchased from Sigma. It was isolated from a rough *E. coli* strain F583. This monolayer was patchier than the lipid A monolayer formed with the head out. The monolayer was flatter than either of the monolayers formed with the rough or smooth strains. There were no domains similar to those present in the rough LPS monolayers in the lipid A monolayer. However, there are domains present but they were not of a similar size, shape, or consistency. It is possible that the same phenomenon that cause the domains in the rough LPS monolayers. It is also possible that there is poor coverage of the mica. There was no bumpiness in the lipid A monolayer as seen in the smooth LPS monolayers.

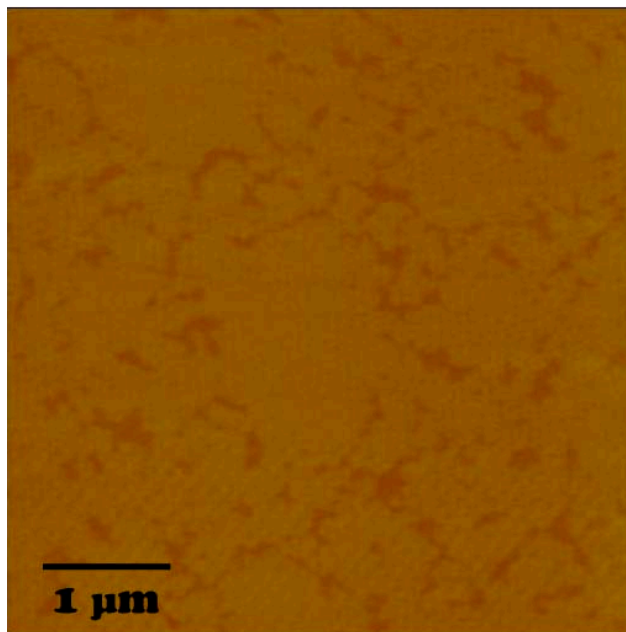


Figure 27: Image of a lipid A monolayer made with the fatty acid tails facing out. This image is of a monolayer made from lipid A purchased from Sigma and isolated from a rough strain *E. coli*, F583. The tails of the lipid are facing out. This image measures 5  $\mu\text{m}$  by 5  $\mu\text{m}$  and has a z scale of 10 nm. This was the best image of all the images obtained of these monolayer. This image has been flattened.

## CHAPTER 4: DISCUSSION

### Section 1: Bdellovibrio Cultivation

Bdellovibrios were observed using both light microscopy and atomic force microscopy. Their growth was further characterized by monitoring the number of prey left during each day of a four day growth cycle. Light microscopy showed to what extent the bdellovibrio were feeding on their prey. The bdellovibrio have a distinct swimming pattern from the prey cells and are easily identified. The prey cells have a vibrating motion as they slowly float through the culture, moving in only one direction. The bdellovibrios have a more purposeful swimming motion; they tend to move in straighter lines and various directions. They are seen swimming quickly through the culture, bumping into other cells along the way. The bdellovibrios are also much smaller than the prey cells.

Examining bdellovibrio cultures with a light microscope did not give us detailed images of the growth. AFM was used to observe the bdellovibrio growing inside its prey. After examining with AFM many filters prepared with prey and bdellovibrio culture under AFM, only *E. coli* cells were visible. There were a few possible bdelloplasts but not as high as might be expected. There were also no free swimming bdellovibrio. I determined that it would be

beneficial to change the strain of *E. coli* from the original AB1157 to ML35. When observing the filters, the *E. coli* AB1157 observed were also very small and this may have affected the ability of the bdellovibrios to grow inside this strain of prey as bdellovibrio growth is affected by the size of their prey. It is also possible that the *E. coli* were so hardy that they could grow quickly in the adverse conditions that they were placed in. Any size constraints were alleviated by changing to strain ML35, which has been used very effectively in the past, and bdelloplasts were readily visible when filters were prepared with bdellovibrio culture and ML35 prey suspension.

Initially, even with the prey change, the bdellovibrio did not take over. This might be caused by the fact the bdellovibrio cultures were not growing continuously, and keeping a culture growing may allow the bdellovibrios to become stronger. Bdellovibrio requires specific conditions for growth such as a temperature no warmer than 30°C and a sugar concentration not greater than 10%. The bdellovibrio must also have a continuously aerobic environment and must also find a prey cell in which to grow before it metabolizes all its biomolecules. By providing the ideal environment for growth, the health of the bdellovibrio culture improved. Growth of the bdellovibrio cultures was greatly increased once the sugar concentration of the final nutrient broth was decreased. Once the nutrient broth was correct, the bdellovibrio, when observed with a light microscope, had taken over a culture in three days.

While the AFM provides detailed images of the bdellovibrio growing, it cannot provide quantitative data on bdellovibrio growth and predation. Prey cell counts were used to provide a quantitative approach to determine bdellovibrio growth. Because bdellovibrio requires specialized growth conditions (as described above) and takes a long time to form a plaque, measuring the number of prey cells in the suspension can be used as an indirect method to quantitate bdellovibrio growth. The fewer prey cells that are growing in suspension, the more bdellovibrio predation is occurring. This technique may allow us to draw some valuable conclusions on the relationship between bdellovibrio predation and the LPS structure of the prey cell. It may be that bdellovibrio have a higher rate of predation for rough strains than they do for smooth strains. This might be because the smooth strains have O-antigens above the lipid A moiety, and if the bdellovibrio is recognizing the lipid A, the O-antigens could present a barrier to bdellovibrio recognition. In rough strains, which have no O-antigens, the lipid A is more accessible to the bdellovibrio. This could result in a higher rate of bdellovibrio predation of rough strains which would be measured as a decrease in the number of prey cells in the bdellovibrio culture.

Unfortunately, when trying to monitor the growth of the bdellovibrio by counting the number of prey cells left, the bdellovibrio did not dramatically reduce the number of K12 and O111:B4 prey cells. Bdellovibrio were visible swimming through each suspension when viewed with a light microscope, but

their presence was not represented in the growth curves of the O111:B4 or K12. We believe that the bdellovibrio were not growing well because they were started in suspension from a frozen stock suspension and they were not happy with the change of prey. If growth curves were measured again for O111:B4, ML35, K12, and ZK1056 with a bdellovibrio suspension that had been growing on the prey for a given time in ideal conditions, we could calculate accurate numbers of prey cells in the suspension and construct an accurate growth curve. This would allow us to determine if bdellovibrio has a higher rate of predation for rough or smooth strains.

## **Section 2: LPS Extraction and Purification**

The LPS extraction process is not an easy one. It involves several steps over the course of a week: two or three extractions, a dialysis, and two or three long centrifugations. All these steps separate the DNA, phospholipid, and protein components and allow for the LPS to be isolated for further use. Before we started the extraction procedures, it was important that we develop a method to measure the amount of LPS, protein, and DNA in each step of the process. Several methods were given a trial run with standard LPS and DNA solutions. First, Thin Layer Chromatography (TLC) was performed with the standard LPS sample and a DNA solution using a variety of different solvents composed of varying amounts of methanol, chloroform, water, and acetic acid, but the separation of various components was quite poor. The LPS

would either remain at the origin or travel with the solvent front. The LPS and DNA never separated on the TLC plate. This failure to separate these two seemingly different molecules is indicative of the similarities in the physical properties of these two molecules, which is elaborated below. The best TLC results were obtained with isolated lipid A, which is what the protocol was originally intended for, indicating that this method may prove useful for comparing the lipid A of the extracted LPS.

Secondly, a carbocyanine dye used to detect and quantitate LPS and DNA. Stains-All, or 1-ethyl-2-(3-(1-ethyl-naphtho(1,2 d)-thiazolin-2-ylidene-2-methylproprenyl)naphtho(1,2 d)-thiazolium bromide, which has been used to determine LPS content in earlier studies (45), was used to observe the UV/Vis spectrum of LPS in comparison to a DNA solution. This technique was difficult to utilize in a timely and efficient manner. LPS has a very weak peak at 270 nm, which is similar in wavelength though not molar absorptivity to the strong DNA peak at 280 nm. In theory, the dye shifts the LPS peak to around 400 nm. Sometimes the dye blank would not work properly, and any LPS or DNA peak would be lost in a large peak that covered most of the spectrum. The major problem was the light sensitivity of the dye. The absorbance of the blank was continually changing and if any standard peaks were present they would shift depending on the dye. A new batch of dye had to be mixed every 2 hours. This meant that the spectrophotometer needed to be recalibrated to the fresh dye sample, leading to a change in the intensity of

the standard peaks. While the spectra that were obtained for the LPS standards provided some information, it was not as valuable as that obtained from other methods.

In the third method, electrophoretic gels were run with the LPS standards and stained with silver to detect LPS. Though this process did take some time, both to run the gel and then stain it, and the staining process was not always reproducible, even poorly stained gels gave more valuable information than the two previous methods. Therefore we choose to continue to use this method to characterize all of the LPS samples.

The set of three gels measuring the amount of DNA, protein, and LPS, have not only confirmed the composition of the final samples as LPS but have also monitor the presence of each molecule present in each step of the extraction process. The first set of gels, run with samples taken from each step of the extraction process performed with the *E. coli* ML35, lead us to modify the procedure. In this extraction there is no appreciable increase in the amount of LPS obtained between the second and third extraction. However there is extra DNA present in the third extraction. Because of this observation that the third extraction does not improve the yield but decreases purity, the third extraction was not performed in the subsequent LPS extraction procedures of ZK1056, bdellovibrio, K12, and O111:B4. There is no change in the amount of DNA lost between the second and third centrifugation steps and this centrifugation increases the likelihood that some of the LPS are lost

in the supernatant of the third centrifugation. Because there was no detectable removal of DNA and there is a possibility that some of the LPS could be lost, the third centrifugation step was eliminated in the following four extractions. The silver stain also stained some protein as well, so it is important to run at least a protein gel for comparison during an extraction process to make sure there is no extra protein carried through out the process that could be misidentified as LPS.

These extraction processes illustrate some interesting similarities and differences in the physical properties of each biomolecule. In the extraction, differences in polarity were exploited to move the protein into the phenol while leaving the DNA and LPS in the aqueous solution. Many of the proteins have large hydrophobic areas that are normally contained in the hydrophobic lipid bilayer of either the inner and outer membrane or have a core of hydrophobic amino acids that are normally contained in the core of the proteins. These hydrophobic areas, which are much greater than that of the LPS molecules, are what causes the protein presence in the phenol layer. Most would not consider the LPS and DNA molecules to be similar enough to be kept in the same aqueous extraction phase. The amphipathic nature of the LPS molecule is such that the LPS molecule segregates into the aqueous phase along with the hydrophilic DNA rather than in the phenol with the protein. The other lipids, which don't have the added hydrophilicity of the core and O-antigens, will also segregate to the phenol layer.

While this removes the protein, the DNA and LPS must still be separated from each other. This similarity in hydrophobicity does present a slight problem in separating these two molecules. However the molecules have a different enough hydrophilicity to exploit. While the molecules are similar enough to both be present in the aqueous phase of the extract, the DNA is more hydrophilic than the LPS because of its larger charge. When centrifuged at high forces the LPS will come out of aqueous solution while the DNA stays in. Large pieces of DNA are more readily precipitated from an aqueous solution than smaller pieces of DNA and it is the large pieces of DNA that are present in any of the final LPS products.

Based on these gels and the monolayers made from the final LPS solutions, it appears that no further purification beyond centrifugation was needed. While there is some DNA and perhaps a small amount of protein in the final extracted solution, we propose it is present in such low amounts that any DNA or protein would not affect the final monolayers. The protein was present in such a low concentration that it did not even show up on the protein gel. Any DNA left in the solution has a very high molecular weight as shown by the fact that the DNA stayed close to, if not in, the well. However, any DNA that is present does not seem to affect the LPS monolayers. No DNA is present in any of the AFM scans of any of the LPS monolayers made on the silanated glass. This suggests that because the cover slip is so hydrophobic and DNA is so hydrophilic, any DNA present in the final solution will not

stick to the alkylated surface. No DNA is present in any of the AFM scans of the LPS monolayers made on mica either. As in the monolayers formed on glass, the DNA does not stick to the mica. Both the mica and the DNA are negatively charged. We are confident that the final product is sufficiently pure and will form consistent monolayers.

### **Section 3: LPS Characterization**

The most important information about the LPS molecules was obtained from the electrophoretic gels stained to detect LPS. Similar techniques to those used to monitor the extraction procedure were also used to obtain information about the LPS standards, but again the polyacrylamide gel gave the best results and was used for further study. These gels, though also difficult to perfect, have yielded valuable information about both standard and extracted samples. Even though Figure 16 shows only six of the eight samples and is not extremely well separated, there is a plethora of information contained in this gel. The first lane shows the commercially obtained O111:B4 standard and the second lane is the remainder of that sample. The appearance of the LPS in these lanes look similar to the LPS that is present during the O111:B4 extraction process (Fig. 15c), which means that they have the same overall structure. This similarity means that the LPS is not degrading during the extraction process. Further characterization of the extracted sample will show that the standard and the extracted samples stain in

the same way, specifically in a way similar to that seen in the remainder lane of Figure 16. With better separation in the gel we will even be able to identify how many repeating O-antigen units the O111:B4 contains. From the remainder lane we can already see the LPS banding and at least four bands are visible with a large unresolved band at the top. These bands mean that there are at least five, and likely more, repeating O-antigen units. The fact that the bands showed up in the overflow lanes means that the resolution of each O-antigen repeating unit is concentration dependent and lowering the concentration of the sample will increase the separation of each band.

Information about the ML35 and *bdellovibrio* LPS is also available from Figure 16. Lane 3 contains the extracted ML35 sample and lane 4 contains the extra sample not put into the main lane. Lane 5 contains the *bdellovibrio* sample. Based on this gel, both of these LPS samples were extracted from smooth strain bacteria and appear to be fairly similar to each other, though the ML35 is better resolved than the sample from the *bdellovibrio*. This similarity may occur because the two LPS samples have a similar LPS structure. Alternatively, the *bdellovibrio* might incorporate whole LPS molecules from the ML35 prey cells and use them in its own outer membrane. It is also possible that there are contaminant ML35 LPS molecules in the *bdellovibrio* preparation. If the third possibility is true, we should be able to separate any prey LPS by precipitating the unique *bdellovibrio* LPS in ethanol based on the work of Schwudke *et al.* (25). The

banding in the ML35 overflow lane shows five bands along with a large undifferentiated band at the top. These bands mean that the ML35 LPS contains at least five repeating O-antigen units, and probably more due to the undifferentiated band. Since at this time the gel does not contain any well resolved bands for the *bdellovibrio* LPS, no conclusions can be drawn as to the number of O-antigen units contained in the LPS molecule. The *Pseudomonas aeruginosa* LPS seen in lanes 8 and 10 showed no separation but did have undifferentiated band at the top of the gel consistent with a smooth strain.

As seen in Figure 16, both the ZK1056 and the EH100 clearly have only one undifferentiated band at the bottom of the gel. This presentation is consistent with a rough strain LPS, which EH100 is known to be. This single band has led us to conclude that the ZK1056 is also a rough strain which was not known before. We predict that the K12 LPS should appear similar to the ZK1056 and the EH100 as the K12 is another known rough strain.

From these gels alone, the designation (either rough or smooth) of each LPS sample has been determined. The *Pseudomonas aeruginosa*, O111:B4 (both standard and extracted), ML35, and *bdellovibrio* LPS are all smooth strains. The ZK1056, K12, and EH100 are all rough strains. Further characterization should provide more detail about the structure of the LPS molecules, especially about the number of repeating O-antigen units on the smooth strains.

#### Section 4: Supported LPS Monolayers

In theory, AFM should be able to image a surface on the nanometer molecular scale. In this work, the molecular scale is not necessarily the most useful. The consistency and continuity of the monolayer is most important and must be observed using a larger scan size. Most scans were taken in a 5  $\mu\text{m}$  by 5  $\mu\text{m}$  square. Larger scans were also used, especially when trying to form a hole in the monolayer. Compared to other work with LPS monolayers, such as that of Roes *et al.* (39), these images are at least four times the size of other scans. While a larger scan size might make it more difficult to capture a perfect image, it is a better measure of the consistency of the monolayer. A smaller size scan might make a good image easier to find, but it does not offer as strong a support of a uniform surface. Smaller scan scales might be used in the future to further investigate the composition of our supported LPS monolayers.

In order to determine if a LPS supported monolayers has been formed, the clean glass and the alkylated glass first had to be characterized. The clean glass was not completely flat at the 10 nm scale but that is to be expected as glass is actually a liquid. It was impossible to keep the glass clean when it was transported in the AFM room from Petri dish to microscope and thus there was some dust that attached to the glass, especially on the alkylated glass. Dust particles or other dirt may have some effect on how the monolayers form, especially if the alkylated glass has been sitting for a while.

However if the glass substrate has been freshly alkylated, there should be minimal contamination.

The mica did not seem to have the same problem with dust as the alkylated glass did, probably due to the fact that the surface was not treated with something hydrophobic. The surface of the mica was completely flat when imaged at the 10 nm scale. Mica is flat at a molecular level which explains why it appears so much flatter than the glass.

It was possible to conclusively determine that there were LPS monolayers formed when LPS molecules were inoculated onto an alkylated cover slip. Each monolayer appeared well formed when imaged with AFM. If the areas that were observed did not have a layer of LPS covering it, the tip would not be able to make contact with the extremely hydrophobic surface underneath. The presence of imperfections was also helpful in determining the presence of a monolayer on the rest of the surface. Imperfections were most frequent when making LPS layers by vesicle fusion, which tends to make bilayers instead of monolayers. It may be that the alkylated cover slips need to sit longer in the LPS solution to produce a more evenly coated surface. With the dipping method, there were fewer imperfections but there were more liposomes. This may be because the liposomes left over from preparing the LPS solutions were attracted to the LPS molecules that had formed the monolayer on the cover slip. However it is very easy to remove

the liposomes; simply running the AFM tip over the area removed the liposomes from the surface into the fluid.

There were no obvious differences between the images of the “heads-out” monolayers made from the six different types of LPS and lipid A as seen in Figures 20, 22, and 23. The ML35, *bdellovibrio*, *pseudomonas*, and the O111:B4 standard, all smooth strains as determined by gel electrophoresis, have very similar AFM images and very similar appearance in the polyacrylamide gel. The EH100, a known rough strain, and the ZK1056 were expected to produce a different image than the smooth strains; however there was no observable difference between the monolayers formed by the rough and smooth strains. The lipid A, isolated from ML35, showed no difference in the monolayer as well. Based on the results for these other monolayers, the K12 and extracted O111:B4 LPS monolayers formed with the heads out should appear very similar. The only difference in these monolayers would be the height, because each of the LPS molecules is a different height. The smooth strains will have O-antigens while the rough strains and the lipid A have none. However these differences are not readily visible in the AFM images since all the image shows is the surface. It might be possible to determine the height of the monolayer if we could scratch off an area of the monolayer as has been done in other studies with fixed objects (46).

All the monolayers imaged in fluid were very consistent, both in their formation and their observable properties. These monolayers appeared very

fluid. The alkylsilane acts somewhat like an inner leaflet of a bilayer making this a good model membrane. Since it acts as a model membrane it should conform to the fluid mosaic model in which the molecules in a membrane are in constant movement. Proof of this fluidity can be seen when an attempt is made to form a hole in the monolayer. When extra pressure was exerted with the AFM tip to create a permanent hole in the monolayer, the molecules would move back to the scratched area before an image could be taken. The best result is seen in Figure 21, and even in that image there is still a complete monolayer. Since AFM captures images on a large time scale, it is possible that a hole is formed but the speed with which the AFM captures the image is too long and the molecules have moved back into place. In order to create a hole in the monolayer, the tip must scratch through the alkylsilane layer, which has not yet been accomplished because of possibility of damaging the tip. Perhaps then the LPS will not be able to return to the scratched area. It would be interesting to run a fluorescent recovery after photobleaching (FRAP) experiment on these monolayers. We have yet to produce an adequate image of a fluorescent LPS monolayer using fluorescent monolayer. The image has either been too bright or too dim. Once a good monolayer is accomplished for fluorescent imaging, a FRAP experiment could be run to determine if there is a difference in the molecular movement within the monolayer that stems from a difference in the molecular structure of each LPS molecule.

These monolayers were also not completely smooth. This roughness is expected because, not only is the glass underneath not completely smooth, but the molecules themselves vary slightly in length because of the O-antigen. This slight roughness can also be explained because of their fluidity. In the case of the smooth LPS monolayers, the O-antigen chains were able to move in solution, and because the AFM captures images over such a large time scale, the position of the O-antigen chains may not be completely extended into solution, leading to a “rougher” appearance in the monolayer. The LPS molecules may also be interacting with each other to some extent on the molecular scale which generates domains and causes a slightly rougher appearance.

In contrast to those monolayers formed with the heads out, the monolayers formed with the fatty acid tails out show a marked difference between those formed with smooth LPS and those formed with rough LPS. While the formation of monolayers with the tails out might seem like an odd choice because it is not as biologically relevant, these monolayers are much more stable than those imaged in fluid. This stability was seen when an area was imaged repeatedly and there was no drifting. Often in an image of a heads out monolayer with a liposome attached, the liposome would shift position as subsequent images were obtained. Movement of a distinguishable feature did not happen with the monolayers formed with the tails out. If a

liposome was present on the first image, it appeared on subsequent images in the same place.

The smooth LPS monolayers were mostly well covered and each monolayer was similar to the other smooth LPS monolayers. The monolayers formed were somewhat rough in appearance. This could be caused by the difference in size of the individual LPS molecules due to the variability in the number of O-antigens present. Each smooth LPS molecule will have slightly different lengths which may be shown as roughness in the surface.

The rough LPS monolayers were extremely different than those formed by the smooth LPS. The rough LPS formed monolayers with odd patchy domains. The domains in the EH100 were fairly regular and circular. In the ZK1056, the patches were much less regular, both in size and shape. Where the EH100 were all circular and about 0.25  $\mu\text{m}$  in diameter, in the ZK1056 monolayer the patches were anywhere from about 0.05  $\mu\text{m}$  to 0.5  $\mu\text{m}$  in diameter. In the K12 monolayer, the view is obscured by vesicles that have attached to monolayer, but the background shows only the monolayer and the same patchy domains are clearly visible. These patches are small but are more uniform in size at roughly 0.1  $\mu\text{m}$  in diameter.

Based on the work of Roes *et al.* (39), who also saw this phenomenon in their monolayers formed with rough LPS, these domains are actually areas of higher molecular packing density or "LC". The surrounding monolayer has a lower molecular packing density, or "LE". At this time, based solely on the

images, it appears that we are encountering the same phenomenon here. At this time we do not have the ability to obtain data that either proves or disproves their theory that these domains are of a higher molecular packing. Hopefully a Langmuir-Blodgett trough will aid in these investigations and allow us to make that determination. The reason that each rough LPS monolayer looks different from the others must be due to something in the molecular structure but at this time we can not determine what part of the molecule establishes how these monolayers form. It is, however, reassuring that all the rough strains that we have observed form similar monolayers. These monolayers have also confirmed that the monolayer observed by the Gutschmann research group was not specific to the LPS they used. We also hope that the rigidity of these monolayers will allow us to determine the height of the monolayers by scratching a hole and measuring the distance from the mica to the surface.

## CHAPTER 5: CONCLUSIONS AND FUTURE WORK

### Section 1: Conclusions

Here we show that we can successfully extract and purify LPS from various bacteria strains. The final product contains minimal amounts of protein and DNA, and any DNA that is present does not have any effect on the monolayers that the LPS form. We can also characterize this LPS using a polyacrylamide gel stained with silver salts. We now know that the *P. aeruginosa*, O111:B4, ML35, and bdellovibrio LPS all contain O-antigens and are thus smooth. We also know that the EH100, K12 and ZK1056 do not have O-antigens and are thus rough.

We have used our extracted LPS to form two types of monolayers. The monolayers formed with the heads out are very fluid and appear very similar. The monolayers formed with the tails out are very different depending on whether the LPS are rough or smooth. The rough strain LPS monolayers form domains which may have a higher molecular packing density than the surrounding monolayer.

Now that we have successfully characterized monolayers composed of isolated LPS from the relevant bacteria, we need to make higher quality and more consistent monolayers using a Langmuir-Blodgett trough. The trough

will let us control the molecular packing and allow us to monitor the isotherms of each LPS species. These monolayers will be imaged in the same way, but we will be able to monitor the formation more quantitatively. We hope that the information from the Langmuir-Blodgett trough will indicate whether there are differences in the molecular structure that change the pressure under which the phase transitions of the monolayer occurs. We expect to see a noticeable difference in the isotherm of the monolayers formed by *Bdellovibrio* LPS based on the work of Schwudke *et al.* (25) in which the *Bdellovibrio* strain that they worked with, HD100, had a lipid A moiety that contains neutral sugar groups where the prey lipid A contains phosphate groups. If lipid A structure of *Bdellovibrio bacteriovorus* 109J is similar to that of HD100, this change in structure from charged to neutral should be reflected in the isotherm of the *Bdellovibrio* monolayer.

Along with the Langmuir-Blodgett monolayers, we hope to further characterize parts of the LPS using Gas Chromatography/Mass Spectrometry (GC/MS). In order to analyze such a complex biomolecule, the molecule must be broken up into pieces. GC/MS would specifically be used to look at the fatty acid tails and head groups of the lipid A molecule, following a procedure similar to those of Schwudke *et al.* (25) and Muller-Loennies *et al.* (29). We would expect to find that there is a difference in the structure of the lipid A head group of the *Bdellovibrio* LPS as compared to its prey, probably a

replacement similar to the mannose that replaced the phosphate groups in the *Bdellovibrio bacteriovorus* HD100.

Eventually, we expect to use fluorescent microscopy to monitor bdellovibrio binding affinity to each LPS monolayer. In order to accomplish this we will need bdellovibrios that express the GFP plasmid. We have an electroporation method that we hope will yield a fluorescent bdellovibrio culture. Once we have the fluorescent bdellovibrio, we can use fluorescent microscopy to monitor the number of bdellovibrio that irreversibly bind to the monolayer after a given period of time. Perhaps then we can conclude whether the LPS molecule, specifically the lipid A, is the molecule that bdellovibrio recognizes in the irreversible binding step of the growth cycle.

## References

- (1) Stolp, H., and Starr, M. P. (1963) *Bdellovibrio bacteriovorus* gen. et sp. n., a predatory, ectoparasitic, and bacteriolytic microorganism. *Antonie van Leeuwenhoek* 29, 217-248.
- (2) Ruby, E. G. (1991) The genus *Bdellovibrio*, in *The Prokaryotes: a handbook on the biology of bacteria: ecophysiology, isolation, identification, applications* (Balows, A., Truper, H. G., Dworkin, M., Harder, W., and Schleifer, K.-H., Eds.) pp 3400-3415, Springer-Verlag, New York.
- (3) Straley, S. C., LaMarre, A. G., Lawrence, L. J., and Conti, S. F. (1979) Chemotaxis of *Bdellovibrio bacteriovorus* toward pure compounds. *J. Bacteriol.* 140, 634-642.
- (4) LaMarre, A. G., Straley, S. C., and Conti, S. F. (1977) Chemotaxis toward amino acids by *Bdellovibrio bacteriovorus*. *J. Bacteriol.* 131, 201-207.
- (5) Straley, S. C., and Conti, S. F. (1977) Chemotaxis by *Bdellovibrio bacteriovorus* toward prey. *J. Bacteriol.* 132, 628-640.
- (6) Abram, D., e Melo, J. C., and Chou, D. (1974) Penetration of *Bdellovibrio bacteriovorus* into host cells. *J. Bacteriol.* 118, 663-680.

- (7) Starr, M. P., and Baigent, N. L. (1966) Parasitic interaction of *Bdellovibrio bacteriovorus* with other bacteria. *J. Bacteriol.* *91*, 2006-2017.
- (8) Koval, S. F., and Bayer, M. E. (1997) Bacterial capsules: no barrier against *Bdellovibrio*. *Microbiology* *143*, 749-753.
- (9) Burnham, J. C., Hashimoto, T., and Conti, S. F. (1968) Electron microscopic observations on the penetration of *Bdellovibrio bacteriovorus* into gram-negative bacterial hosts. *J. Bacteriol.* *96*, 1366-1381.
- (10) Varon, M., and Shilo, M. (1968) Interaction of *Bdellovibrio bacteriovorus* and host bacteria. *J. Bacteriol.* *95*, 744-753.
- (11) Thomashow, M. F., and Rittenberg, S. C. (1978) Intraperiplasmic growth of *Bdellovibrio bacteriovorus* 109J: solubilization of *Escherichia coli* peptidoglycan. *J. Bacteriol.* *135*, 998-1007.
- (12) Tudor, J. J., McCann, M. P., and Acrich, I. A. (1990) A new model for the penetration of prey cells by bdellovibrios. *J. Bacteriol.* *172*, 2421-2426.
- (13) Rittenberg, S. C., and Shilo, M. (1970) Early host damage in the infection cycle of *Bdellovibrio bacteriovorus*. *J. Bacteriol.* *102*, 149-160.

- (14) Cover, W. H., and Rittenberg, S. C. (1984) Change in the surface hydrophobicity of substrate cells during bdelloplast formation by *Bdellovibrio bacteriovorus* 109J. *J. Bacteriol.* *157*, 391-397.
- (15) Tudor, J. J., and Karp, M. A. (1994) Translocation of an outer membrane protein into prey cytoplasmic membranes by bdellovibrios. *J. Bacteriol.* *176*, 948-952.
- (16) Diedrich, D. L., Duran, C. P., and Conti, S. F. (1984) Acquisition of *Escherichia coli* outer membrane proteins by *Bdellovibrio* sp. strain 109D. *J. Bacteriol.* *159*, 329-334.
- (17) Ruby, E. G., McCabe, J. B., and Barke, J. I. (1985) Uptake of intact nucleoside monophosphates by *Bdellovibrio bacteriovorus* 109J. *J. Bacteriol.* *163*, 1087-1094.
- (18) Beck, S., Schwudke, D., Strauch, E., Appel, B., and Linscheid, M. (2004) *Bdellovibrio bacteriovorus* strains produce a novel major outer membrane protein during predacious growth in the periplasm of prey bacteria. *J. Bacteriol.* *186*, 2766-2773.
- (19) Rayner, J. R., Cover, W. H., Martinez, R. J., and Rittenberg, S. C. (1985) *Bdellovibrio bacteriovorus* synthesizes an OmpF-like outer membrane protein during both axenic and intraperiplasmic growth. *J. Bacteriol.* *163*, 595-599.
- (20) Talley, B. G., McDade, J., Ralph L., and Diedrich, D. L. (1987) Verification of the protein in the outer membrane of *Bdellovibrio*

*bacteriovorus* as the OmpF protein of its *Escherichia coli* prey. *J. Bacteriol.* *169*, 694-698.

- (21) Ruby, E. G., and McCabe, J. B. (1988) Metabolism of periplasmic membrane-derived oligosaccharides by the predatory bacterium *Bdellovibrio bacteriovorus* 109J. *J. Bacteriol.* *170*, 646-652.
- (22) Nelson, D. R., and Rittenberg, S. C. (1981) Partial characterization of Lipid A of intraperiplasmically grown *Bdellovibrio bacteriovorus*. *J. Bacteriol.* *147*, 869-874.
- (23) Nelson, D. R., and Rittenberg, S. C. (1981) Incorporation of substrate cell Lipid A components into the lipopolysaccharide of intraperiplasmically grown *Bdellovibrio bacteriovorus*. *J. Bacteriol.* *147*, 860-868.
- (24) Kuenen, J. G., and Rittenberg, S. C. (1975) Incorporation of long-chain fatty acids of the substrate organism by *Bdellovibrio bacteriovorus* during intraperiplasmic growth. *J. Bacteriol.* *121*, 1145-1157.
- (25) Schwudke, D., Linscheid, M., Strauch, E., Appel, B., Zahringer, U., Moll, H., Muller, M., Brecker, L., Gronow, S., and Lindner, B. (2003) The obligate predatory *Bdellovibrio bacteriovorus* possesses a neutral Lipid A containing  $\alpha$ -D-mannoses that replace phosphate residues. *J. Biol. Chem.* *278*, 27502-27512.

- (26) Beveridge, T. J. (1999) Structures of Gram-negative cell walls and their derived membrane vesicles. *J. Bacteriol.* *181*, 4725-4733.
- (27) Van Amersfoort, E. S., Van Berkel, T. J. C., and Kuiper, J. (2003) Receptors, mediators, and mechanisms involved in bacterial sepsis and septic shock. *Clinical Microbiology Reviews* *16*, 379-414.
- (28) Fomsgaard, A., Freudenberg, M. A., and Galanos, C. (1990) Modification of the silver staining technique to detect lipopolysaccharides in polyacrylamide gels. *J. Clin. Microbiol.* *12*, 2627-2631.
- (29) Muller-Loennies, S., Lindner, B., and Brade, H. (2003) Structural analysis of oligosaccharides from lipopolysaccharide (LPS) of *Escherichia coli* K12 strain W3100 reveals a link between inner and outer core LPS biosynthesis. *J. Biol. Chem.* *278*, 34090-34101.
- (30) Kondakov, A., and Lindner, B. (2005) Structural characterization of complex bacterial glycolipids by Fourier transform mass spectrometry. *Eur. J. Mass Spectrom.* *11*, 535-546.
- (31) Karibian, D., Deprun, C., and Caroff, M. (1993) Comparison of Lipids A of several *Salmonella* and *Escherichia* strains by 252Cf plasma desorption mass spectrometry. *J. Bacteriol.* *175*, 2988-2993.
- (32) Sackmann, E. (1996) Supported membranes: scientific and practical applications. *Science* *271*, 43-48.

- (33) McConnell, H. M., Watts, T. H., Weis, R. M., and Brian, A. A. (1986) Supported planar membranes in studies of cell-cell recognition in the immune system. *Biochim. Biophys. Acta* 864, 95-106.
- (34) Langmuir, I. (1917) The constitution and fundamental properties of solids and liquids. II. Liquids. *J. Am. Chem. Soc* 39, 1848-1906.
- (35) Blodgett, K. B. (1935) Films built by depositing successive layers on a solid surface. *J. Am. Chem. Soc* 57, 1007-1022.
- (36) McConnell, H. M., and Brian, A. A. (1984) Allogenic stimulation of cytotoxic T cells by supported planar membranes. *Proc. Natl. Acad. Sci. USA* 81, 6159-6163.
- (37) Koenig, B. W., Krueger, S., Orts, W. J., Majkrzak, C. F., Berk, N. F., Silverton, J. V., and Gawsrisch, K. (1996) Neutron reflectivity and atomic force microscopy studies of a lipid bilayer in water adsorbed to the surface of a silicon single crystal. *Langmuir* 12, 1343-1350.
- (38) Rinia, H. A., and de Kruijff, B. (2001) Imaging domains in model membranes with atomic force microscopy. *FEBS Lett.* 504, 194-199.
- (39) Roes, S., Seydel, U., and Gutschmann, T. (2005) Probing the properties of lipopolysaccharide monolayers and their interaction with the antimicrobial peptide polymyxin B by atomic force microscopy. *Langmuir* 21, 6970-6978.
- (40) Martin, M. O. (2004) Personal Communication (Nunez, M. E., Ed.).

- (41) Westphal, O., and K, J. (1965) Bacterial lipopolysaccharides, in *Methods in Carbohydrate Chemistry* (Whistler, R. L., Ed.) pp 83-91, Academic Press, New York.
- (42) Laemmli, U. K. (1970) Cleavage of structural proteins during the assembly of the head of bacteriophage T4. *Nature* 227, 660-685.
- (43) Tsai, C. M., and Frasch, C. E. (1982) A sensitive silver stain for detecting lipopolysaccharides in polyacrylamide gels. *Anal. Biochem.* 119, 115-119.
- (44) Sambrook, J., and Russell, D. W. (2001), Cold Spring Harbor Laboratory Press, Cold Spring Harbor.
- (45) Janda, J., and Work, E. (1971) A colorimetric assay of lipopolysaccharides. *FEBS Lett* 16, 343-345.
- (46) Kelley, S. O., Barton, J. K., Jackson, N. M., McPherson, L. D., Potter, A. B., Spain, E. M., Allen, M. J., and Hill, M. G. (1998) Orienting DNA helices on gold using applied electric fields. *Langmuir* 14, 6781-6784.